VALIDATION OF CURRENT MODERATE RESOLUTION IMAGING SPECTRORADIOMETER (MODIS) DAILY SNOW ALBEDO PRODUCT AND SPATIAL ANALYSIS BASED ON MULTIPLE SENSORS

A Thesis

by

PANSHU ZHAO

Submitted to the Office of Graduate Studies of
Texas A&M University
in partial fulfillment of the requirements for the degree of

MASTER OF SCIENCE

May 2012

Major Subject: Geography

Validation of Current Moderate Resolution Imaging Spectroradiometer (MODIS) Daily Snow Albedo Product and Spatial Analysis Based on Multiple Sensors

VALIDATION OF CURRENT MODERATE RESOLUTION IMAGING SPECTRORADIOMETER (MODIS) DAILY SNOW ALBEDO PRODUCT AND SPATIAL ANALYSIS BASED ON MULTIPLE SENSORS

A Thesis

by

PANSHU ZHAO

Submitted to the Office of Graduate Studies of
Texas A&M University
in partial fulfillment of the requirements for the degree of

MASTER OF SCIENCE

Approved by:

Chair of Committee,	Andrew G. Klein
Committee Members,	Anthony M. Filippi
	Ping Yang
Head of Department,	Vatche P. Tchakerian

May 2012

Major Subject: Geography

ABSTRACT

Validation of Current Moderate Resolution Imaging Spectroradiometer (MODIS) Daily Snow Albedo Product and Spatial Analysis Based on Multiple Sensors. (May 2012)

Panshu Zhao, B.A., Nanjing University of Posts & Telecommunications

Chair of Advisory Committee: Dr. Andrew G. Klein

Snow albedo is one of the most important factors for atmosphere-surface energy exchange in high latitude areas. Remote sensing provides continual observations of snow albedo. However, the reliability of snow albedos obtained from remotely sensed images can be problematic, especially when acquired over heterogeneous land surfaces.

This research examines spatial variations in snow albedo observed under different conditions in order to assess how accurate an individual *in situ* observation of snow albedo is when compared to the Moderate Resolution Imaging Spectroradiometer (MODIS) daily snow albedo product (MOD10A1) and its relationship with land surface types. In addition to the field observations, albedos retrieved from two SURFRAD stations are also examined. The overall Root Mean Square Error (RMSE) between the *in situ* and MODIS albedos is 8%.

Semivariogram analysis of Landsat ETM+ snow albedo retrievals on January 26th, 2010 over an ice and snow covered lake indicates spatial autocorrelation lengths of approximately 260 m, suggesting limited *in situ* observation can be considered fairly representative of albedos retrieved from MODIS images. To further reveal what

parameters could influence the spatial representativeness, this research examined landscape metrics based on seven binary snow maps created from Landsat images for three areas of differing roughness and for different snow cover conditions. There are two Landscape metrics, Mean Shape Index (MSI) and Area Weighted Shape Index (AWMSI), were found to be correlated the spatial autocorrelation lengths of snow albedo as measured from the range distance of the modeled semivariograms.

In addition, this research also introduced a method of using multi-angle mast to measure the surface bidirectional reflectance distribution function (BRDF). This method could be used for further research to build the BRDF library of the snow-covered canopies.

ACKNOWLEDGEMENTS

I would like to thank the Texas A&M University Geography Department for the great academic environment. I would also like to thank my committee for their support of this project. In particular, I would like to thank Dr. Andrew Klein for guiding every step of this project. I would also like to thank Dr. Anthony Filippi for tutoring me in the fundamental remote sensing course and *GIS Modeling*; and Dr. Ping Yang for the informative *Atmospheric Physics* course.

Thanks also to the students in the *Studies of the Cryosphere* research group who patiently listened to the details of this project and provided helpful feedback.

Finally, thanks to my family for their sincere encouragement and financial support.

TABLE OF CONTENTS

Page

LIST OF FIGURES

FIGURE Page

FIGURE Page

LIST OF TABLES

1. INTRODUCTION

1.1 Importance of Snow Albedo and MODIS Albedo Research

Albedo is the ratio of the reflected solar radiance from a unit surface area into the entire viewing hemisphere to the incident solar radiance, when the surface is under the illumination of a directional beam (Schaepman-Strub et al., 2006). The albedo of the Earth land surface can be highly variable, ranging from 0 to 100%.

In the Earth system, the energy budget keeps the Earth in a stable equilibrium as the energy absorbed by Earth is balanced by the energy reflected from Earth. Thus, land surface albedo plays an important role in Earth's energy balance because it impacts the earth's radiation budget which has the capacity to further effect on biospheric and climatic processes (Hahmann et al., 1995; Lofgren, 1995). Snow is one of the Earth's most quickly changing surface covers and is an important component in the Earth's climate system. It is especially important in controlling the exchange of energy between the surface and atmosphere in the seasonally and permanently snow-covered areas of the Earth. Snow albedo is a critical parameter that influences the energy and mass balance over snow covered surfaces (Klein & Stroeve, 2002).

The albedo of high latitudes is very variable, both in time and space. The albedo of fresh snow normally exceeds 90% while dirty ice albedo can be as low as 20% (Warren, 1982; Oerlemans & Knap, 1998). These differences in snow and ice are influenced by many factors, such as snow and ice grain size, type, impurity, snow and

---

This thesis follows the style of *Remote Sensing of Environment.*

ice distribution, surface roughness, and irradiance characteristics. (Warren, 1982; Aoki et al., 2007; Jin et al., 2008; Dozier et al., 2009).

Currently, measuring snow albedo from space is an emerging research topic. Remote sensing has provided the way for environment monitoring, resource management, and decision making of global climate change and upcoming disasters etc. (Li et al., 2009).

Remote sensing offers a reliable way to determine snow albedo at local to global scales and is the only practical method to measure global surface albedo (Liang, 2001). In general, remote sensing enables the retrieval of direct albedo estimates from satellite images using several approaches. For example, the current Moderate Imaging Spectroradiometer (MODIS) snow albedo algorithm employs multiple steps in its albedo retrieval (Klein & Stroeve, 2002).

MODIS is a remote sensing instrument that is especially suitable for observing the Earth's snow- and ice-covered high latitude regions. MODIS is a currently-operating Earth Observing System (EOS) facility instrument that is available aboard two satellites—TERRA and AQUA in sun-synchronous orbits. Terra MODIS crosses the equator approximately at 10:30 AM while Aqua has a 1:30 PM equatorial crossing time. These satellites provide a global view of Earth's surface every one to two days and acquire multiple images of the Earth high latitudes every day. MODIS acquires information in 36 spectral bands with spatial resolution ranging from 250m to1km. However, only seven bands with resolution of 250m and 500m are suitable for land surface studies (NASA MODIS web: http://modis.gsfc.nasa.gov/about/). The National

Snow and Ice Data Center (NSIDC) Distributed Active Archive Center (DAAC) provides several snow cover products processed from MODIS data (Klein and Barnett, 2003).

An accurate snow albedo product has many potential uses and users. Because snow cover changes rapidly (Klein & Stroeve, 2002) and because it represents a seasonally important water reservoir, it has a large influence on the Earth's water cycle during winter and spring (Dozier et al., 2008). Any algorithm capable of accurately tracking changes in snow albedo has the potential to improve predictions of snowpack development and predictions of snowmelt runoff in hydrological models. At the societal level, accurate albedo estimates can lead to correct climate-change conclusions for both citizens and decision makers. *In situ* measurements in remote sensing are normally used for calibrating the information derived from the remote sensing sensors or for performing unbiased accuracy assessment of the final output of remote sensing (Jenson, 2007). In this research, the *in situ* observations are used for quantitatively validating the current MODIS albedo product and furnishing additional information such as temperature and snow cover extent which aid in the interpretation of MODIS snow albedo retrievals.

Snow cover is a rapidly changing land surface cover which can influence the local climate condition and further influence the global climate. Accurate albedo estimates are required for climate change studies. Therefore, the validation of the current albedo algorithm is both necessary and imperative. Some validation studies of the MODIS albedo algorithm have already been undertaken. Research by Stroeve et al

(2006) found an average root mean square error (RMSE) difference between MODIS and *in situ* observations on the Greenland ice sheet to be approximately 7% (Stroeve et a*l*., 2006). However, validation of the algorithm in other settings and future refinement of the algorithm are still warranted. In addition, in this research spatial analysis is used to examine the spatial representativeness of surface albedo measurements and how they relate to MODIS snow albedo retrievals. This is a creative and crucial research area that has been neglected to date.

1.2 Study Purpose and Objectives

This research investigates the methods to validate the existing MODIS snow-albedo algorithm used to estimate snow albedos from images collected by MODIS. Multiple methods are used to validate snow albedo estimates and examine the spatial representativeness of snow albedos derived from multiple remote sensing sensors. In addition, a method for using multi-angle mast to measure the surface bidirectional reflectance distribution function (BRDF) is discussed.

This research has three objectives. The first is to validate the MODIS albedo product using two approaches, i.e. *in situ* measurements and station measurements. The second is to investigate the spatial representativeness of snow albedos over relatively homogeneous areas using multiple remote sensing inputs in order to assess the appropriateness of using these areas to validate MODIS snow albedo retrievals. The third is to develop a method for using a multi-angle mast and spectroradiometer to measure snow surface and canopy BRDF, aiming at improving the treatment of canopy BRDF in future research.

1.3 Study Area

The study site for this research is Dickenson County in Northwestern Iowa. Within Dickenson County, most areas are under cultivation which is very typical of Midwestern States. Because this county has low relief with extensive farms and sparse forests, it is a very ideal validation site for low resolution satellites, such as MODIS. In 2003, a field validation was conducted by Klein and there is a good agreement between MODIS snow albedo product and *in situ* measurements (Klein, 2003).

The topography and related soils of northwestern Iowa and Dickenson County is dominated by glacial topography associated with past glaciations. In the study region the dominant landform regions are Northwest Iowa Plains and Des Moines Lobe (Fig. 1). In this research, the study area of Dickenson County lies on the western margin of the Des Moines Lobe and its topography ranges from flat glacial till to hummocky moraines.

Big Spirit Lake (Fig.2) is located at 43°27′57″N and 95°6′9″W in Dickinson County, Iowa. This major lake covers approximately an area of 23 km^2 extending 9.6 km north/south and 6.4 km east/west. Its average depth is around 5.2 m with a maximum recorded depth of 7.3 m. Big Spirit Lake normally freezes at the end of November and thaws at beginning of April.

In order to examine the spatial representativeness of one single *in situ* measurement, two terrestrial domains (labeled as d1 and d2) were examined in addition to Big Spirit Lake. These three sites are of different underlying surfaces which could contribute to different spatial attributes of *in situ* measurements. Within the Dickenson County, the dominant topography near the Des Moines Lobe's western lateral margin is the rolling knob-and-kettle terrains (e.g. d1). The relief of more central portions is quite low (e.g. d2). When snow-covered, the three areas are very ideal for validating low resolution satellites (e.g. MODIS) because of their homogeneous land-covers and characteristic topography.

In this study, Spirit Lake is the major site for snow albedo validation. In addition to the lake, d1 and d2 are two areas for investigating the spatial representativeness of snow albedos.

From January 29th to January 31st, 2010, a field validation of snow albedos using different instruments was conducted on the surface of the frozen lake by the Cryosphere Research Group at Texas A&M University. The methods and results will be addressed in this thesis.

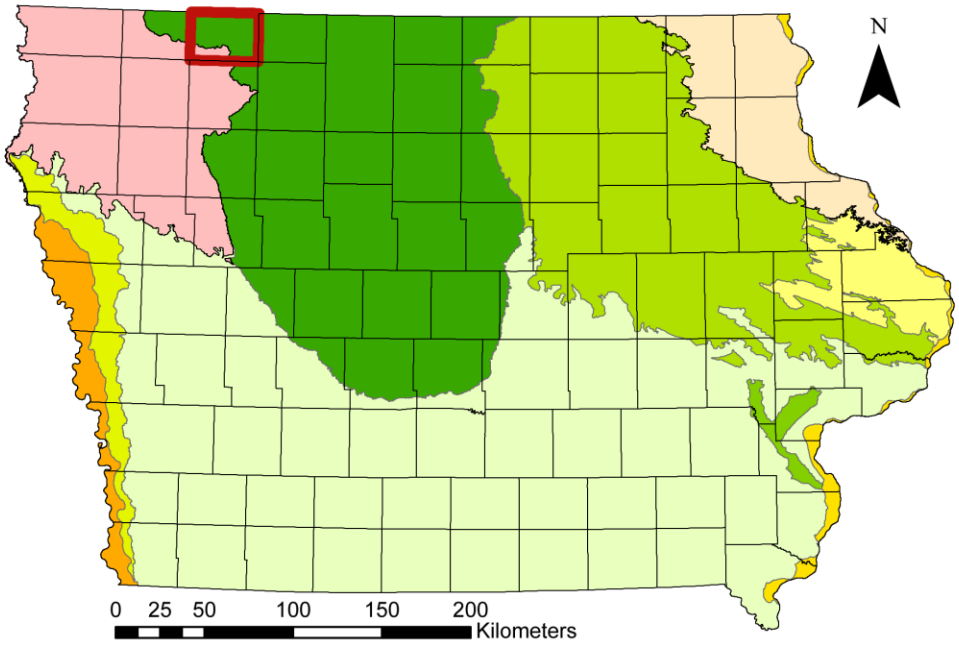

Fig. 1. The Dickenson County, Iowa. It is the study area which is in the red box. The dominant landform region in Dickenson County is Des Moines Lobe (area in dark green color) and the other landform region is Northwest Iowa Plains (area in pink color).

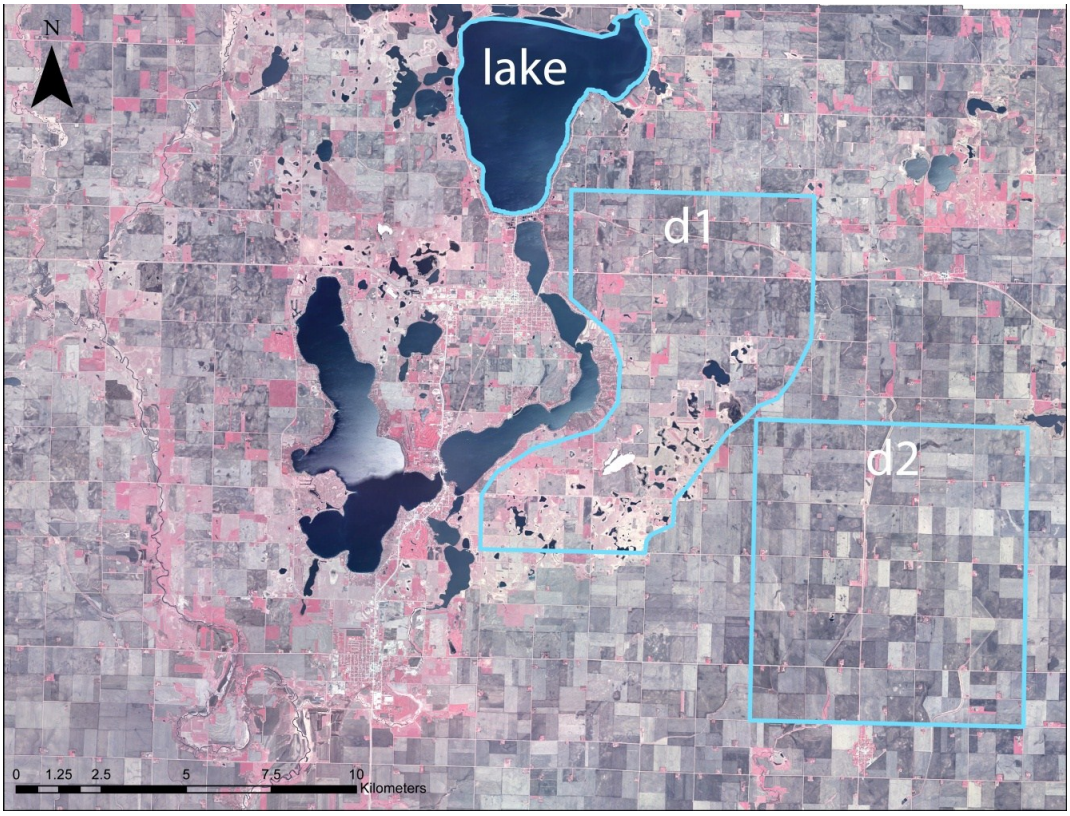

Fig. 2. The aerial photographs of Dickenson County. The blue boxes indicate the threes specific areas for examining the spatial representativeness of snow albedos. The underlying topographies of these three areas vary considerably. The frozen lake is very flat while domain 1 (d1) is rougher than domain 2 (d2) due to different underlying geomorphologies.

2. LITERATURE REVIEW

2.1 The Current MODIS Daily Albedo Product

2.1.1 Background

There are currently many methods for estimating surface albedos (Liang, 2001). Initially, many General Circulation Models (GCMs) have employed non-remote sensing methods to estimate global albedo. Early approaches simply assigned average albedo value to different landcovers (e.g. Dorman & Sellers, 1989), however, remote sensing provides the opportunity for continual observations of snow albedo.

Snow albedo can be retrieved from many satellite sensors, including ASTER, AVHRR, GEOS, ETM+/TM, POLDER, MODIS, Vegetation, etc. (Liang, 2001). MODIS is a very applicable sensor to retrieve snow albedo as its wide swath width allows it to view the world's snow covered regions on a near daily basis.

Before retrieving an albedo from a satellite observation, an atmospheric correction must be applied to reduce the effects of the intervening atmosphere (Jin et al., 2003). For the current MODIS snow albedo algorithm, this is accomplished by using the atmospherically corrected reflectance MODIS Surface Reflectance Product (MOD09) (Vermonte & Kotchenova, 2008; Schaepman-Strub et al., 2006). This product provides standard atmospheric correction for subsequent standard MODIS land surface products (Klein & Stroeve, 2002; Stroeve et al., 2006).

2.1.2 Bidirectional Reflectance Distribution Function (BRDF)

The most challenging part of using satellite images to retrieve albedo is correcting this atmospherically corrected reflectance for anisotropic reflectance. A satellite only senses energy from the surface for a small solid viewing angle (Fig. 3) but albedo is the integration of reflectance over all viewing angles (Ranson, et al., 1994). As a result, the treatment of bidirectional reflectance distribution function (BRDF) should be carefully undertaken.

BRDF is a four-dimensional function that defines how light is reflected from a surface given the orientation of the surface to the sun and the sensor. Because satellites only measure a small portion of the energy reflected from a surface (i.e., the fraction of reflected incident irradiation at a small solid angle), it is necessary to correct this observed reflectance from a solid angle to retrieve albedo. As different viewing angle can lead to different reflectance, BRDF is dependent upon both viewing and solar angles (Lucht et al. 2000).

In theory, if light falling on a surface is scattered to an observer so that its apparent brightness is the same regardless of the observer's angle of view, this surface is a Lambertian surface. Technically the surface luminance of a Lambertian Surface is isotropic. For example, unpolished wood exhibits roughly Lambertian reflectance (Lucht et al. 2000).

However, in nature few, if any, Lambertian surfaces exist and ignoring anisotropic effects can lead to large errors in albedo estimates (Stroeve et al., 1997).

Correcting anisotropy to derive albedo, correction factor must be calculated. The anisotropic reflection function (ARF) provides a method to calculate a correction factor:

$$f(\theta_0, \theta, \varphi_a, \varphi) = \pi \cdot R(\theta_0, \theta, \varphi_a, \varphi)/a_s(\theta_0) \quad (1)$$

where f is correction factor, R is BRDF which varies according to different surface types, and a_s is relative to spectral albedo. In addition, θ_0 is the solar zenith angle, θ is the reflectance zenith angle, φ_a is the solar azimuth angle towards north and φ is the viewing azimuth angle towards north.

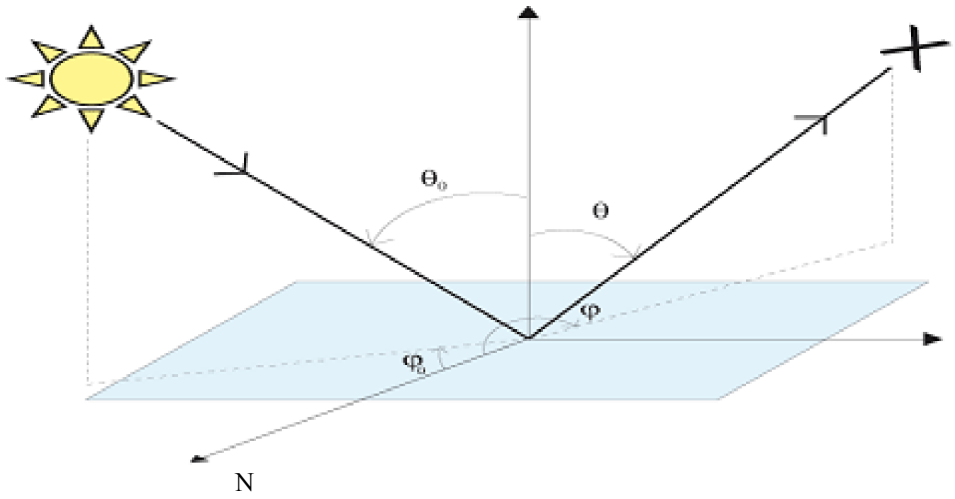

Fig. 3. Viewing geometries. This is the viewing geometry surface location illuminated by the sun and viewed from a satellite.

Currently, there are two MODIS albedo products that retrieve surface snow albedos; these are MODIS 16-day albedo product (MOD43B3) and MODIS daily snow albedo product (MOD10A1). The MOD43B3 employs a "kernel-driven" linear BRDF model, which relies on the surface reflectance measured over a 16-day period. The

MOD10A1 simply uses the semi-empirical model (i.e. DISORT) to model snow BRDF (Stroeve et al., 2002; Stroeve et al., 2006). The temporal resolution of MOD43B3 is sixteen days which is not sufficient to precisely monitor important natural processes occurring within a snowpack such as melting. For this reason, the MODIS daily snow albedo product (MOD10A1) is the preferred product used conducting climate research (Stroeve et al., 2006).

2.1.3 The Performance of MOD10A1

Several validation studies of the MODIS daily snow albedo product (MOD10A1) have documented that this product is suitable over large and flat areas. Stroeve et al (2006) used data retrieved from five Greenland Climate Network Automatic Weather Stations (AWS) to assess the performance of MOD10A1 on the Greenland ice sheet during the summer of 2004. They found there is a general agreement of the MODIS measurements with the station data. The root mean square error (RMSE) for MOD10A1 was 0.067, which suggest this product works well. Hall et al (2009) compared the MODIS daily snow albedo product with the MODIS 16-day snow albedo product over the Greenland Ice Sheet and revealed there is a good correspondence between them, especially in the lower elevation areas of Greenland Ice Sheet.

Although MOD10A1 performed well, the reliability of snow albedos obtained from remotely sensed images can be still problematic, especially if acquired over heterogeneous land surfaces or complex terrains (Sorman et al., 2006). Tekeli et al (2006) examined MOD10A1 product in the mountainous area of Turkey and found this

product overestimated the snow albedo around 10% when compared to the *in situ* measurements.

2.1.4 MOD10A1 Algorithm

As this research investigates the MODIS snow albedo product (MOD10A1), a brief description of the algorithm follows. The snow albedo algorithm for MODIS has been designed and is described in detail in Klein and Stroeve (2002). This algorithm provides daily albedo measurements of the Earth's snow covered surfaces under cloud-free conditions. In order to highlight the problems with the current algorithm, the algorithm is illustrated in Fig. 4 and the approach used is briefly described as follows.

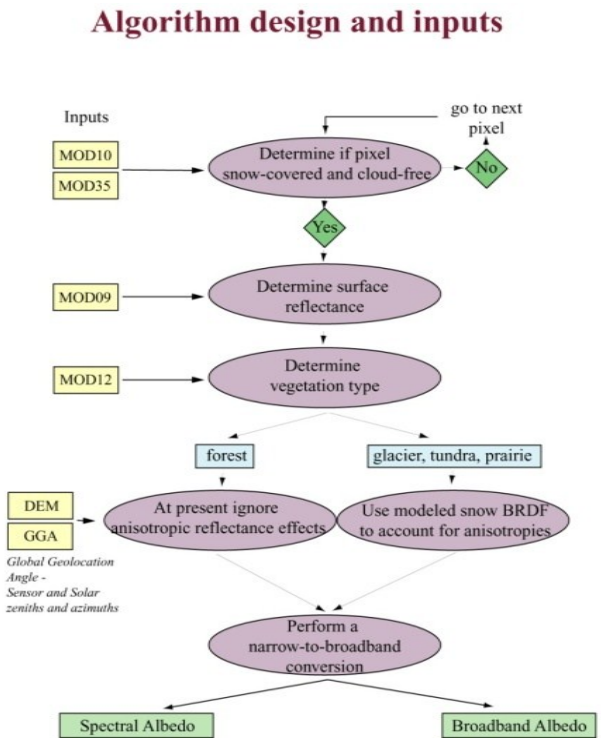

Fig. 4. Flow chart of current MODIS daily snow albedo algorithm. From Klein and Stroeve (2002).

The first step in estimating a snow albedo is to determine if a pixel is cloud free or not, as surface albedo can only be measured in cloud free pixels (Ricciardelli et al., 2010). To distinguish the cloud free pixels, one of MODIS product (MOD35) is applied at the beginning of the algorithm. The existing MODIS cloud mask (MOD35) is designed to do this and flags pixels as cloud-free or cloud-covered (Frey et al., 2004). Once a pixel is determined to be cloud-free, then the MODIS snow-mapping algorithm (MOD10) is used to determine whether each cloud-free pixel is snow covered or snow free.

In the current algorithm, the ARF correction is made using a discrete-ordinate radiative transfer approach (DISORT) that was designed by Stamnes et al (1998) and has been used extensively to model snow BRDF (Klein & Stroeve, 2002). However, this approach cannot successfully model the BRDF of snow-covered forests. Therefore in the existing algorithm, the BRDF of these areas has been simply assumed as Lambertian and no anisotropic correction is done for snow in forested areas.

Because most multispectral satellites only use discrete intervals of wavelength (i.e. bands), it is necessary to convert spectral albedo (i.e. narrowband albedo) to broadband albedo (Liang et al., 2003). The final step of this algorithm is to realize the narrowband to broadband conversion. In the algorithm, the conversion coefficient was developed by Stroeve and Klein (2002).

2.1.5 Progress in Measuring Surface BRDF

In nature, solar irradiance is composed of three components: (1) the direct radiation from the sun, (2) the diffuse radiation which is scattered by the atmosphere

(clouds, aerosols, and gases) and (3) the reflection from surrounding surfaces of the observation. In return, the atmospheric parameters, topography, and the reflectance properties of the topography contribute greatly to both the spectral magnitudes and spectral distributions of the diffusion.

To derive an albedo, accurate BRDF model is required for both explaining and predicting the spectral and directional properties of a target (Liang, 2004). In the current MODIS daily albedo product, the major disadvantage of using DISORT to correct the anisotropic influence is that DISORT is only applicable in places where the dominant landcover is snow. However, in mid to high latitude regions, snow-covered forests are a common landscape, thus the current ARF correction is only suitable for non-forested areas (Klein & Strove, 2002).

Although there are many suitable BRDF models for estimating most surfaces' albedo, most are unsuitable when deriving albedo from very complicated surfaces, such as snow-covered forests. Currently, the BRDF models used for remote sensing are not applicable for snow-covered forest canopies, although there are some BRDF models that can be used for non-snow forests (Wu *et al*., 1995). The scattering properties of snow covered canopy are extremely complex due to many factors, such as leaf orientation, the proportion of snow in the instantaneous field of view of the sensor (IFOV), etc. (Manninen & Stenberg, 2009).

In addition to modeling BRDF, it is also possible to measure it directly. In recent decades, multiple viewing geometry sensors and instruments have been used for measuring surface BRDF (Milton et al., 2009). Satellite sensors, such as Multi-Angle

Imaging Spectrometer (MISR) and Compact High Resolution Imaging Spectrometer (CHRIS) have the capacity to measure surface reflectance in different angles. In addition, for *in situ* measurement, a goniometer is a typical instrument designed for measuring surface reflectance at desired viewing angles (Peltoniemi et al., 2005). However, because satellite sensors are limited by their temporal resolution and the rapidity of snow melting, and because most current goniometers are not high enough to measure the tree canopy (e.g. pines), these methods are not ideal for measuring BRDF of snow-covered forests.

The field spectroradiometers are first designed for the study of human color vision in early 1960s (Penndorf, 1956). The successive development enables scientist to make accurate measurements of the surface's spectral reflectance in nature. The first portable field spectroradiometer was known as the Portable Field Reflectance Spectrometer (PFRS) which significantly influenced and promoted the developments in this area (Goetz, 1987). Alex Goetz and Brian Curtiss subsequently established the company named as Analytical Spectral Devices (ASD Inc.) and currently ASD is a leading manufacturer of field spectroradiaometers (Curtiss & Goetz, 1994).

Currently the field spectroradiometers are often hand-held in order to make measurements. To minimize the scattered light from operator's body, the sensors are normally mounted at a high and/or suspending position (Kimes et al., 1983). It is especially challenging to measure accurate reflectance from tall vegetations, not only because of the difficulties of suspending and operating the instruments, but also because the IFOV could be very complicated and mixed with other undesired elements. In recent

years, to acquire the field spectral data, many innovative ideas have been made, such as kites, balloons, aircraft and even helicopters (Milton et al., 2009). Although these new techniques greatly broaden the ability for field spectroradiometry, they are still not ideal for near-ground measurement. To get the desired intrinsic directional reflectance characteristics of the observed surface, it is better to minimize the disturbance of atmosphere.

2.2 Geostatistics and Landscape Metrics

A large problem encountered in validating low resolution satellites is to understand how representative the *in situ* observations are of, i.e. whether the whole area is covered by IFOV on the ground. Ideally, *in situ* measurements adequately sample variations within the pixel. In addition, as remote sensing images are retrieved instantaneously from the surface, all the ground measurements should be undertaken simultaneously. In reality, validation is successively done by making several field observations (Yu et al., 2010). Another feasible solution is to use images of much higher spatial resolution to examine the corresponding area in low resolution images (Liang et al., 2004). As point observations seemed unsuitable for comparison with MODIS images of 500 m over heterogeneous surfaces, Liang (2002) downscaled Landsat Enhanced Thematic Mapper Plus (ETM+) derived albedo at 30 m into 500 m spatial resolution of MODIS in order to compare to MODIS albedo. The validation results show it is reasonable to use ETM+ albedo to validate MODIS albedo.

However, the question remains of how representative an *in situ* albedo observation is of a MODIS pixel, in other words, how much albedo varies spatially

within one MODIS pixel. Because each pixel in remote sensing images contains the spatial information for the entire area to its location, it is possible to examine the spatial variations by using a finer resolution images in each MODIS pixel, such as ETM+ (Walsh et al., 1999).

It is necessary to examine both variations in snow albedo and landscape metrics to ascertain over what distance snow albedo can be considered spatially auto-correlated (i.e. within what distance one *in situ* measurement can be considered representative) as well as to further demonstrate whether or not using one point observation to validate MODIS albedo is spatially representative.

Geostatistics provides a method to describe these spatial variations in snow albedo. Kriging is a geostatistics method to quantitatively examine the spatial dependence of natural resources. The geostatistical techniques were first proposed by Matheron (1971) and were expanded to the study of soil science to investigate the regionalized variables (Curran, 1988). Kriging is a spatial interpolation method which is based on statistical models that consist of spatial autocorrelations. There are two major tasks involved in the kriging process and these are quantifying the spatial structure of the surrounding data points and producing a prediction at a new location. Therefore, kriging not only offers a way to predict a surface according to available observations, but also provides criteria to assess the accuracy of spatial interpolation (Krige, 1951).

Autocorrelation depicts the statistical relationship among observation points, so the correlation is not only confined by the distance but also by the direction separating the locations. In kriging, the autocorrelation can be examined by a semivariogram which

depicts the relationship between semivariance and distance. In spatial statistics, semivariance is calculated as one-half of the squared difference between each pair of points at different distances (Longley et al., 2004). The semivariogram is usually calculated by the following equation:

$$\gamma(\mathrm{h}) = \frac{1}{2}(\mathrm{N} - \mathrm{h}) \sum_{\mathrm{i}=1}^{\mathrm{N}-\mathrm{h}} [\mathrm{Z}(\mathrm{i}) - \mathrm{Z}(\mathrm{i} + \mathrm{h})] \qquad (2)$$

where N is the total number of observation points and i is the location in the specific study area. Each pair of points at the sampling distance h is examined using this equation to calculate the semivariance.

The semivariogram is a good indicator of spatial dependence and spatial variability (Burrough, 1983). According to Tobler's first law of Geography, neighboring places are more similar than the farther apart ones (Longley et al., 2004). Therefore, it is effective to use a semivariogram to check both the spatial scale and resolution effects of landscape properties, as captured by the sampling interval *h*. In general, spatial autocorrelation exists if the semivariance increases as the distance between observations (*h*) increases.

The semivariogram can also help provide information of best sampling interval for *in situ* validations of snow albedos. This can be inferred from the range distance captured from the semivariogram. In a semivariogram, the range is the distance from the origin to the distance (*h*) where the shape of the semivariogram model flattens. The spatial autocorrelation increases within this range while there is no spatial autocorrelation beyond the range. The range distance is the key factor that can reflect the spatial representativeness of landscape properties (Meentemeyer, 1989). Some remote

sensing projects adapt the range distance derived from images to quantitatively identify the optimum spatial resolution (Jenson, 2007). This research investigated the range distances of snow albedo under different snow conditions and different landscapes using high resolution images.

In Landscape Ecology, spatial heterogeneity of land covers and their effects are considered and emphasized in relevant research, such as by examining the habitat fragmentation to evaluate both regional and global biodiversity (Risser et al., 1984; Harris, 1984). To facilitate such research, the Spatial Pattern Analysis Program for Categorical Maps (FRAGSTATS) was developed by Dr. McGarigal and Barbara Marks of Oregon State University to quantify the spatial structure of landscapes. Many landscape metrics can be calculated from patch scale to the entire landscape scale (McGarigal et al., 1995), however, in this research, the landscape parameters of mean shape area index and area weighted mean shape area index were found to best represent the shape complexity of both patches and landscapes (Burrough et al., 1986; Mandelbrot et al., 1982; Milne et al., 1988) and are thoroughly investigated.

The Mean Shape Index (MSI) is calculated by the following equation in FRAGSTATS:

$$\mathrm{MSI} = \frac{\sum_{j=1}^{n}\left(\frac{0.25 p_{ij}}{\sqrt{a_{ij}}}\right)}{n_i} \qquad (3)$$

where i is the number of classes, j is the number of patches, n and n_i are the number of patches in the landscape class, p_{ij} is the perimeter (m) of patch ij, a_{ij} is the area (m^2) of patch ij.

The Area Weighted Shape Index (AWMSI) is used to give each patch a weighting of its area size. The equation is:

$$\text{AWMSI} = \sum_{j=1}^{n}\left[\left(\frac{0.25p_{ij}}{\sqrt{a_{ij}}}\right)\left(\frac{a_{ij}}{\sum_{j=1}^{n} a_{ij}}\right)\right] \quad (4)$$

Both MSI and AWMSI are unity (1) when all patches are perfectly square and increase in value as the patch shapes become more irregular (McGarigal, 1995).

This research uses geostatistical methods to examine the spatial representativeness of MODIS daily snow albedo product (i.e. MOD10A1) by the aid of finer images (i.e. Landsat). FRAGSTATS is used in this research for computing relevant landscape metrics for spatial patterns (UMass Landscape Ecology Lab). The semivariogram is examined in detail to characterize the strength of the spatial dependence of the albedo. In addition, this research also investigates what factors can affect the spatial-autocorrelation lengths for snow albedo in the studied terrain (Brown et al., 1993).

3. METHODS

To investigate the accuracy as well as to validate the MODIS daily snow cover product provided as part of MOD10A1 suite, albedos retrieved from *in situ* measurements and station measurements were examined in this research. To investigate if point observations of snow albedo can be considered be spatially representative of an area approximating a MODIS resolution (500 m) pixel, geostatistics were used to examine the spatial scales over which of snow albedos are found to be spatially autocorrelated for differing snow cover conditions and over relatively homogeneous, but topographically variable terrain. As the current MODIS daily snow albedo poorly modeled the BRDF of snow-covered canopies, a method using multi-angle mast to measure canopy BRDF is also discussed.

3.1 Accuracy Assessment of the Current MODIS Snow Albedo Algorithm

In situ measurement of snow albedo is a necessary tool for validation of remote sensing products, such as the MODIS snow albedo product. Validation of snow albedo retrievals from a large footprint sensor like MODIS benefits from both point and areal measurements of snow albedo. This section describes the *in situ* data collection method to validate the current MOD10A1 daily snow albedo product.

3.1.1 Comparisons to *In Situ* Estimates of Snow Albedo

A major question in the validation of satellite observations, especially for low spatial resolution instruments like MODIS, is how accurately does an individual or limited number of point observations characterize the instantaneous field of view (IFOV)

- the “footprint” observed by a satellite? For these considerations it is important to characterize a large area to adequately describe a satellite footprint. To facilitate validation of the MODIS snow albedo product, a field campaign was undertaken.

The field campaign took place in northwestern Iowa with albedo measurements made on the frozen Spirit Lake from February 29th to 31th, 2010. Statistical analysis was performed to assess how well the collected observations characterized the albedo of a MODIS pixel. To assess the accuracy of the MODIS snow albedo retrievals, further analysis was achieved by comparing MODIS retrieved albedos to the point validation data sets described above. The snow albedo estimates were calculated using the existing MODIS algorithm. This provided important information on whether or not the retrieved MODIS albedos are of sufficient accuracy to be useful to the wider scientific community.

Two types of pyranometers (i.e. photodiodes and thermopiles) were used to measure snow albedo in the field. Inexpensive photodiodes only cover a limited spectral region (typically 300-1000 nm) but are robust under field conditions. Thermopiles cover broader wavelength regions than photodiodes, but are both more expensive and more

fragile. Therefore, the expensive thermopiles are suitable for measuring at a fixed location while the photodiodes are better suited for repeated moving to measure albedoin different geographic locations. In this research, two instruments were used in field for snow albedo validations; these are Middlteon-EP16 pyrano-albedometer and LI-COR 200SA pyranometers. LI-COR pyranometers are a typical photodiode instrument while EP16 is thermopiles instrument. These two instruments are different not only in cost and quality, but also in durability.

Incoming solar radiation covers the electromagnetic spectral region from 300 nm to 3000 nm. The Middleton EP16 nominally measures solar radiation over the 300 to 3000 nm wavelength regions (Klein, 2003).The LI-COR is an inexpensive solution for measuring radiation but only measures the wavelength region between 300 nm and 1100

Table 1. A comparison between EP16 and LI-COR pyronometers.

	EP16	**LI-COR**
Spectral Ranges	300nm-3000nm	300nm-1100nm
Price	5500 USD	440 USD

nm. However, it has been demonstrated that snow albedo measurements obtained from LI-COR instruments are comparable with the thermopile type pyranometers under clear sky conditions (Stroeve et al., 2001; Stroeve et al., 2002). Considering their durability and cost (Table 1), the EP16 is normally used as a bench mark when validating the snow albedo while LI-COR is frequently moved around.

Clear skies, below 0°C temperatures, and adequate snow cover are the three requisite components for successful snow albedo validations. The metrological conditions were met when this field work was conducted during three days in the late January 2010. On January 29th, these two albedometers were set up at the center of Spirit Lake at the position of the green dot in Figure 5. To examine the feasibility of using the LI-COR pyranometers for validating MODIS daily albedo measurements, and also in order to perform a comparison between different instruments, the EP16 and LI-COR instruments were put facing towards each other over same surface for 40 minutes as shown in Figure 6.

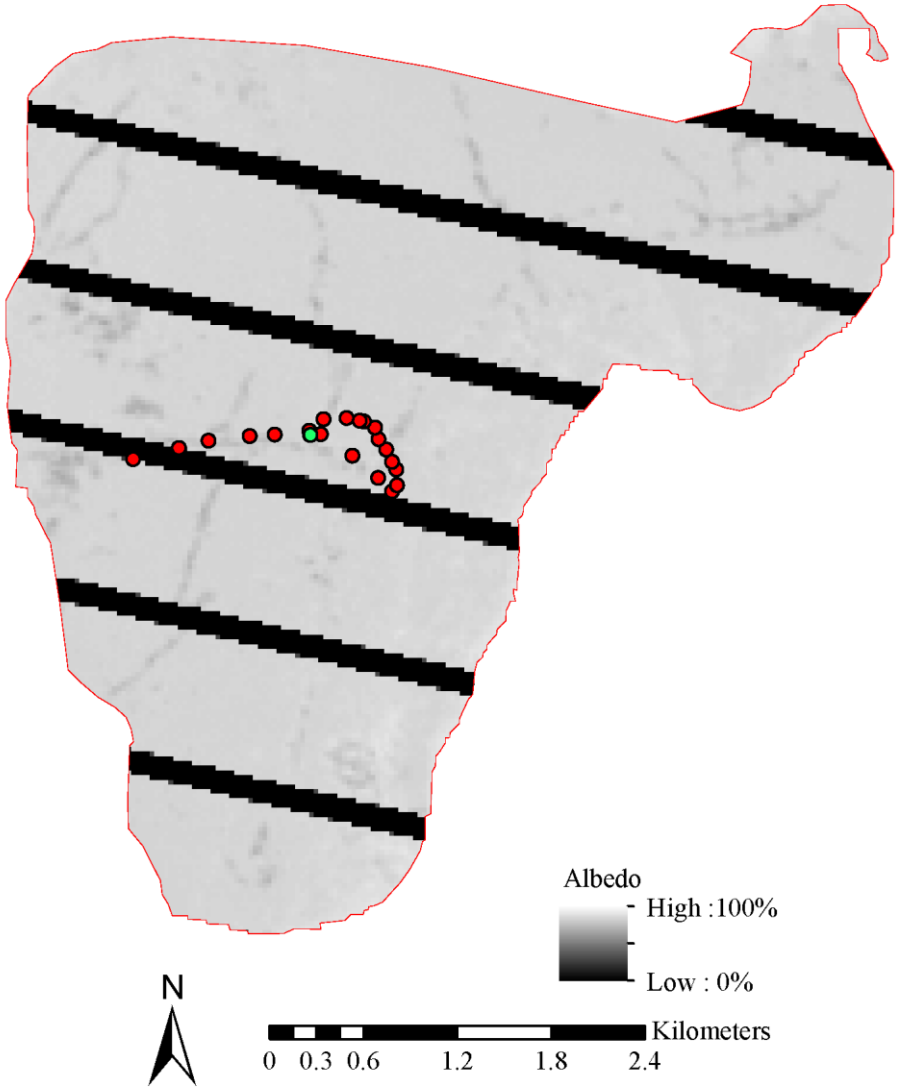

Fig. 5. Landsat albedo map on January 26th. The 22 sites where LI-COR instrument was used for measurement. The base map is an albedo map derived from Landsat ETM+ on January 26th. The green dot is the place where the EP16 instrument was put for three days. The stripes in the image are due to the Scan Line Corrector (SLC)-off.

Fig. 6. EP16 and LI-COR instruments facing to each. The support structures were placed perpendicular to the sunwith the instruments always pointing south of the mounting devices to minimize shadowing effects.

The focus of the 2nd day of field work, January 30th, was to investigate spatial variability in albedo over the lake as the spatial variation of surface albedo was closely related with the lake underlying surface types. On January 30th, the January 29th site was reoccupied by the two albedometers for comparison at the beginning of the day's observation. Then to examine spatial variability in albedo, the LI-COR instrument was deployed at twenty-two sites on the lake. Each of these locations was characterized, in terms of snow depth, ice thickness and a three to five minute integrated albedo

measurement was made. The locations of these twenty-two sites are shown in a Landsat ETM+ albedo map of the frozen Spirit Lake surface from February 26th, 2010 (Fig. 5).

In general all of the albedo measurements sites could be classified into one of two categories: snow or ice. However, there was considerably variation in each of these categories in terms of snow texture, grain size, and surface roughness. Four typical surfaces are illustrated in Figure 7. At each site, albedo measurements were made that each lasted a minimum of 3 minutes following the leveling of the albedometer. Post processing involved elimination of spurious high and low albedos. A mean albedo was then computed from the remaining measurements. Over the course of January 30th, the EP16 was placed at the same location in the lake and recorded albedo continuously over the entire measurement period.

On January 31st, the EP16 was placed at the same site where it had been placed on 29th and 30th and measured for four additional hours. The EP16 albedometer was the only instrument used during all three days, so it was used as a comparison for MODIS-derived albedos.

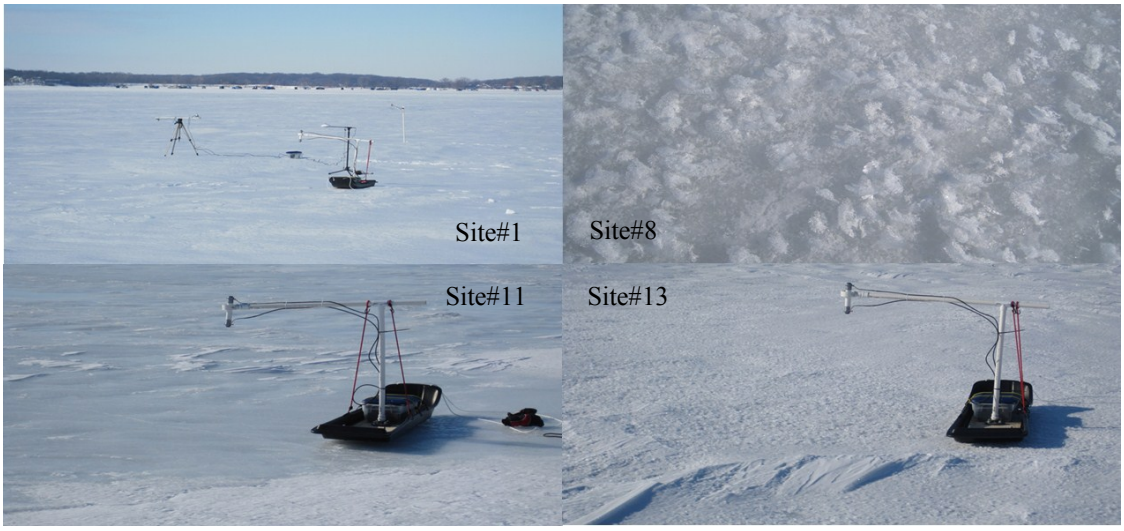

Fig. 7. Four different surfaces over frozen lake. The four typical sites where the underlying surfaces are very different.

3.1.2 Comparisons to *In Situ* Albedo Measurements Made during Snow Season

Surface Radiation Budget Network (SURFRAD) sites are designed to support climatic research by providing an accurate and consistent long-period record of the surface radiation budget at seven stations with the continual observations (NOAA SURFRAD Network). In the conterminous United States seven SURFRAD sites are currently operational: Bondville, IL, Desert Rock, NV, Fort Peck, MT, Goodwein Creek, MS, Penn State, PA, Sioux Falls, SD, Table Mountain, CO. Two additional sites (Barrow, AK and the South Pole) which belong to Baseline Surface Radiation Network (BSRN) were developed by National Oceanic & Atmospheric Administration (NOAA) Global Monitoring Division (GMD) and provide similar measurements of shortwave energy fluxes. At both sets of stations, the upwelling and downwelling radiance (280 nm-3000 nm) are provided by averaging every 3 minutes' measurements.

In this research, two SURFRAD stations located in areas with significant periods of snow were examined in detail — Fort Peck, MT and Barrow, AK (Fig. 8). The land surfaces at these two sites are homogeneous making them ideal to use sites for validating snow albedo retrievals from a large footprint sensor such as MODIS.

Fort Peck (48.31° N, 105.1° W) was established in 1994 and is located on the Fort Peck Tribes Reservation, approximately 15 miles north of Poplar, Montana. The topography at the site is flat and the land cover is short-grass prairie, typically of the northern Great Plains as can be seen in Figure 9 (NOAA SURFRAD network). The Barrow station (71.323° N, 156.6114° W) was established in 1973 and is located near sea level 8km east of Barrow, Alaska. The typical land cover is homogeneous tundra as is illustrated in Figure 10 (GMD observation operations).

As both of these sites are located in the mid- or high- latitudes, there is sufficient snow fall in winter to maintain a snowpack. Each station has continuous terrestrial metrological measures, including temperature, upwelling and downwelling radiance, humility etc. For this study, temperature, upwelling and downwelling irradiance are the properties of interest. As mentioned, albedo was computed by the ratio between upwelling and downwelling radiance.

Fig. 8. Location map of Barrow and Fort Peck. The ARM station at Barrow, Alaska and the SURFRAD station at Fort Peck, Montana were used in this study. The red dots are the Global Monitoring Division (GMD) stations.

Fig. 9. Field view of the Fort Peck, Montana SURFRAD site. It was established in 1994 and is located on the Fort Peck Tribes Reservation, approximately fifteen miles north of Poplar, Montana. (NOAA SURFRAD Network)

Fig. 10. Field view of the Barrow, Alaska ARM site. It was established in 1973 and is located near sea level 8 km east of Barrow, Alaska (GMD observation operations).

In performing validations of MODIS snow albedos, station albedo measurements were compared to the MODIS-derived albedo over the entire snow season for the two hydrological years of 2008 and 2009. Hydrological years run from October 1st to September 1st of the following year.

The MODIS data from Terra satellite used in the study was retrieved from the NSIDC NASA DAAC (National Snow and Ice Data Center Digital Active Archive Center) using the Warehouse Inventory Search Tool (WIST) at https://lpdaac.usgs.gov/lpdaac/get_data/wist. The in *situ* data were retrieved from two different sources: SURFRAD (i.e. surface radiation) Network FTP (ftp://ftp.srrb.noaa.gov/pub/data/surfrad/Fort_Peck_MT/) and Atmospheric Radiation Measurement (ARM) (https://www.arm.gov/).

In determining what daily period of *in situ* observations to compare to the retrieved MODIS albedo, an appropriate time window had to be determined. As the Terra Satellite overpass time for each site was typically at approximately 10:30am local time, a time window running from 10:00 am to 11:00 am local time was selected to average both the *in situ* albedo.

To extract the MODIS albedo the ENVI 4.6 software package was used. The pixel values of two sites of all the images are extracted and documented. For MOD10A1, each pixel is assigned a value as listed in Table 2 (National Snow and Ice Data Center).

In order to further examine the relationship between the MODIS albedo and snow depth, measured snow depth were retrieved from two stations, GGW (Glasgow, MT) and PABR (Post Rogers Memorial Airport, AK), of National Operational Hydrologic Remote Sensing Center. Because there is no snow depth record available in both SURFRAD stations, GGW which is 70 miles from Fort Peck station and PABR

which is 4 miles from Barrow station are the two closest stations with documented snow depth data.

Table 2. MOD 10 A1 data description.

Pixel Value	Meaning
0-100	Snow albedo
101	No decision
111	Night
125	Land
137	Inland winter
139	ocean
150	Cloud
250	missing
251	Self-shadowing
252	Landmark mismatch
253	BRDF Failure
254	No production mask

3.2 Investigating the Spatial Representativeness of Snow Albedos Retrieved from Remote Sensing

The reliability of using field albedo observations for validating albedos retrieved from remote sensing images is constrained by surface heterogeneity. Therefore, it is important to investigate the size of an area for which a point observation can be considered representative. This research employs semivariogram analysis and kriging to investigate the distances over which snow albedos are correlated on the relatively flat and homogenous landscape of northwestern Iowa.

To investigate spatial variability in albedo over spatial scales appropriate to the MODIS sensor, albedos retrieved from higher spatial resolution satellites were used to examine autocorrelation lengths within lower spatial resolution images. In this study, Landsat TM/ETM+ images at a spatial resolution of 30 m were used to investigate spatial autocorrelation in albedo at the spatial resolution on the order of a MODIS pixel which is 250 to 1000 m. This research also examined the representativeness of *in situ* data over different surfaces and regions.

3.2.1 Kriging

The semivariogram quantitatively demonstrates that the nearby observations are more similar, in other words, more spatially autocorrelated than the observations spaced farther apart. A semivariogram offers the ability to measure the strength of statistical correlation as a function of distance. The semivariogram is the key function in geostatistics to examine spatial relationships of the underlying observations. Figure 11 is a typical anatomy of a semivariogram.

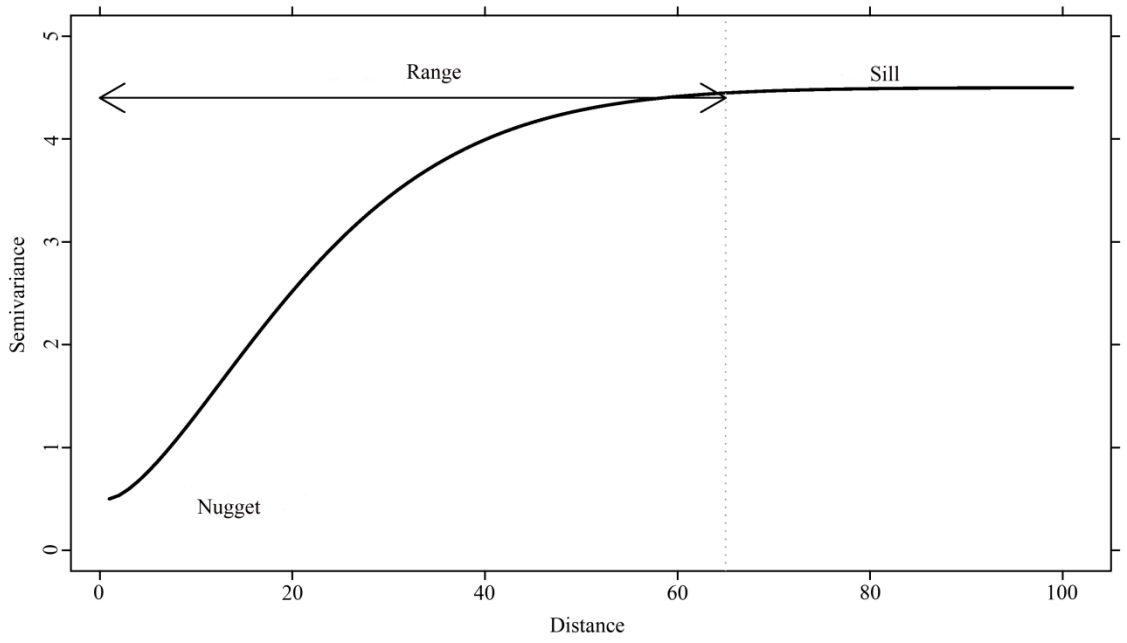

Fig. 11. A typical anatomy of semivariogram (figure from ArcGIS desktop help).

As is shown in Figure 11, several parameters describe a semivariogram. The nugget is the intersection on the y-axis (semivariance) where the fitted trend intersects the x-axis at a distance of 0. The sill is the semivariance where the fitted semivariogram tends to flatten. The range represents the sample distance under which observations can be considered to be spatially autocorrelated. At distances greater than the range distance, observations can be considered to be not spatially correlated.

In reality, it is impossible to calculate empirical semivariogram at every lag distance interval. However, to solve the problem, an applied geostatistics method, such as kriging can be used. Kriging adapts certain model functions to approximate the variation of the semivariance at appropriate lag distances. There are several common

empirical interpolation models including the Gaussian model, Spherical model and the exponential models (Chiles & Delfiner, 1999; Cressie, 1993). In this research the Gaussian model was selected for interpolation.

3.2.2 Data Sources

To examine the spatial representativeness of snow albedo over relatively homogeneous terrains, the Landsat ETM+/TM images required for this study were obtained for the United States Geological Survey's EROS Data Center using its USGS Global Visualization (GloVis) data inventory tool (http://glovis.usgs.gov/). Albedo maps of the three study regions were used for geostatistical analysis, especially for semivariogram analysis.

Two major criteria were considered when selecting appropriate Landsat ETM+/TM scenes for analysis. The first was that the scenes should be representative of different snow-covered conditions over the study area which is highlighted in the red box as shown in Fig. 12. The second criterion was that there should be minimal cloud cover over the study area. Only seven Landsat ETM+/TM images in the EROS archive met these criteria and are listed in Table 3 and illustrated in Figure 12. As Landsat ETM+ and TM sensor have the same spectra response functions, it is applicable to use them together for further analysis (Liang, 2004).

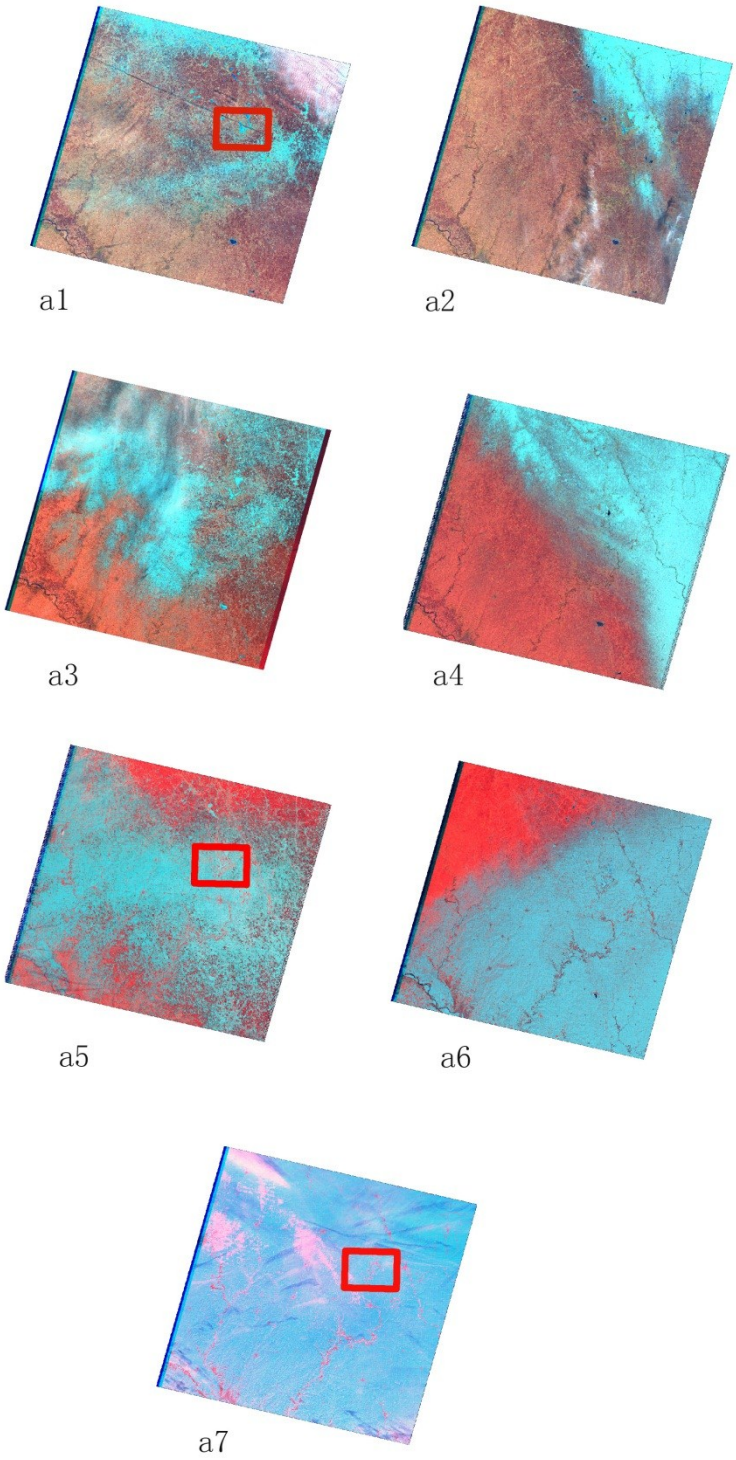

Fig. 12. The seven scenes that were used in this research. These scenes are arranged from patchily snow-covered to fully snow-covered conditions. The red box is the study area.

Table 3. Landsat image information for the seven selected study scenes.

Scene Name	Date	Landsat Sensor
a1	2000-02-16	ETM+
a2	2000-02-24	TM
a3	2002-02-21	ETM+
a4	2006-02-08	TM
a5	2008-03-01	TM
a6	2002-02-05	ETM+
a7	2004-02-03	TM

In Table 3 the seven scenes are ordered according to total snow cover in the scene (see Figure 12) with snow cover increasing from scene a1 to scene a7. The snow condition in the a1 scene is very patchy while it is almost 100% snow covered in the a7 scene.

3.2.3 Processing

To derive the Landsat albedo image, the following preprocessing steps were undertaken, including the standard digital number (DN) to radiance conversion, an atmospheric correction, and a narrowband-to-broadband conversion. The Landsat images were converted to radiance using a standard method (NASA, 2009). The atmospheric correction of each scene employed Fast Line-of-sight Atmospheric Analysis of Spectral Hypercubes (FLAASH) module in the ENVI software package. Finally, a

narrowband to broadband conversion was used to converting spectral albedo to broadband albedo (Liang, 2001):

$$\alpha = 0.356\alpha_1 + 0.130\alpha_3 + 0.373\alpha_4 + 0.085\alpha_5 + 0.072\alpha_7 - 0.0018 \quad (5)$$

where α refers to the broadband albedo value and α_i is spectral albedo in the appropriate Landsat band. The final albedo maps were used for geostatistical analysis, especially for semivariogram analysis.

Albedo images of the study area were first extracted by the corresponding shapefile of borders of each of the three areas (Lake, d1 and d2) and were then converted into point observations for kriging. A normalizing transformation and trend removal are applied at each albedo dataset prior to kriging.

Normalization is done to transform the observations to help them better conform to a normal distribution and the trend removal is to remove any directional trends hidden in the observations (Table 4, Table 5 and Table 6).These steps can both help to increase the accuracy of the interpolation (ESRI Geostatistical Analyst Tutorial)

.

Table 4. The transformations and trend removals of seven lake images.

Lake	Transformations	Trend Removed
a1	Log	1
a2	Log	1
a3	None	1
a4	Log	1
a5	None	1
a6	None	1
a7	None	1

Table 5. The transformations and trend removals of seven d1 images.

d1	Transformations	Trend Removed
a1	Log	1
a2	Log	2
a3	None	1
a4	None	1
a5	None	1
a6	Box-Cox-2	1
a7	Box-Cox-5	1

Table 6. The transformations and trend removals of seven d2 images.

d2	Transformations	Trend Removed
a1	Log	1
a2	None	1
a3	None	1
a4	None	1
a5	None	1
a6	Box-Cox-3	1
a7	Box-Cox-13	1

When interpolating, the Gaussian kriging model was selected using 30 m lag size and encompassing 20 lags, because the Landsat sampling interval is of 30 m and considering 20 lags means the approximate distance under consideration is 600 m which approximates the linear dimensions of a MODIS pixel which is 500 meters. The semivariogram of each interpolation is examined and the range is derived from such semivariogram.

3.2.4 Surface Roughness Detection

Surface roughness is one factor that can potentially lead to variations in snow albedo (Warren, 1982; Aoki et al., 2007; Jin et al., 2008; Dozier et al., 2009). Conceptually, smoother areas may be expected to have smaller variations in snow albedo. Therefore semivariograms of snow albedo over the smoother areas would be expected to have larger ranges as determined from the semivariograms. To examine the influence from surface roughness to different ranges, a 10 meter digital elevation model (DEM) obtained from National Elevation Dataset (NED) was used to quantitatively derive two surface roughness ratios.

A landscape is normally described in terms of planimetric area. However, albedo is spatial dependent on three dimensional characters of the landscape and the slope and aspect of a surface contribute to the variations in surface albedo (Corripio, 2004; Dozier et al., 2009), therefore it makes sense to examine the ratio of planimetric area to surface area as a surface roughness criterion. Surface roughness was derived by the aid of the ArcGIS extension Surface Area and Ratio (Jenness, 2009).

The surface roughness ratio was calculated from the 10m NED DEM and representations of ratio between the surface areas and the planimetric area were computed as they are. The surface roughness ratio is a typical index that represent both the topographic roughness and the convolutedness (Jenness, 2004).

3.2.5 Binary Snow Mapping and Landscape Metrics

To aid in deriving landscape metrics from the studied Landsat ETM+/TM images, binary snow cover extent was also computed to relate to the albedo images

derived from the images. This was done in order to investigate relationships between snow albedo autocorrelation lengths, surface roughness and the patchiness of the snow cover. To create the binary snow cover maps, a version of the current MODIS binary snow mapping algorithm which uses two criteria in combination to differentiate between snow and non-snow areas was used (Hall et al., 1995). The first is a normalized difference snow index (NDSI) value which is greater than 0.40. In addition, only pixels with a reflectance around 0.9 μm (i.e. MODIS band 2 or TM band4) of larger than 11% will be classified as snow (Klein, et al., 1998).

The input data into the algorithm are the seven Landsat spectral bands which are already atmospherically corrected. The output is a binary image in which all the pixels are classified as either snow or non snow. Typically if more than fifty percent of the pixel is snow-covered, a pixel will be classified as a snow pixel (Hall et al., 2002). In this research, MSI and AWMSI are calculated by FRAGSTATS and then examined.

3.3 Developing an Approach to Use a Multi-angle Mast for the BRDF of Snow Covered Surfaces and Canopies

During winter, the albedo of forested area is complex as it consists of both snow and canopy radiative properties (Manninen et al., 2009) and in the current MODIS snow albedo algorithm, the BRDF of forest is poorly modeled (Stroeve et al., 2006). In order to measure surface and canopy BRDF, a tiltable 5 meter mast with a mounted ASD field-portable FieldSpec® Pro Spectroradiometers were constructed by the Geochemical & Environmental Research Group (GERG) at Texas A&M University (Figure 13). The

mast can be extended up to five meters as is illustrated in Figure 14, making it possible to measure the BRDF of snow-covered vegetation.

Here, a procedure for using the instrument to measure snow-covered surfaces and vegetation has been developed to make the most efficient use of the mast-ASD system. It was planned to deploy the instrument during the 2010-2011 snow season, but snow and weather conditions precluded its use, so the device is planned to be used during the 2011-2012 snow season.

Fig. 13. The constructed multi-angle mast. This instrument can help to measures canopy BRDF.

Fig. 14. The top part of the mast. The Pan-Tilt Unit, digital compass and ASD pistol are onboard there.

3.3.1 Instruments

This multi-angle mast instrument is composed of five major components; these are the controllable Pan-Tilt Unit (Model PTU-D46), a digital compass, a five meter mast, and an ASD spectroradiometer and the operation interface which is a laptop computer. The core component is the Pan Tilt Unit developed by Directed Perception Incorporation, which is operated and controlled with Multi-Threaded TTY software from a laptop. Both AC and DC 12-volt power sources can supply the power for operating the Pan-Tilt Unit.

Fig. 15. The ASD spectroradiometer and the controlling devices.

Fig. 16. The structure of the Pan-Tilt Unit. The Pan-Tilt unit can point to specific angles.

3.3.2 Field Usage

As constructed, the system can point the ASD spectroradiometer over a range of the relative azimuth angles (φ) from 0° to 280° and over sensor of zenith angles (θ) from -70° to +70°. To construct a reasonable BRDF, albedo measurements should be collected every 10 degrees in zenith (θ) and 30 degrees in azimuth (φ). The attached digital compass enables precise determination (to within 1°) of orientation of the two viewing directions of the ASD spectrometer.

Because of the way in which the mast system is constructed, it was determined that the most efficient approach was to use the PTU-D46 tilt function to measure at different relative zenith's and its pan function to measure at different relative azimuth angles.

3.3.3 Orienting the System

Using the digital compass which is mounted on the Pan-Tilt Unit, the first step is to set the mast's initial azimuth angle to north (φ), so the recorded azimuth angle measures 0° at the start. It is then necessary to document the angle of the solar principal plane during the time the measurements will be made and then adjust to the mast's viewing azimuth angle to sweep the ASD spectrometer along the principal plane using the PTU-D46's pan axis.

3.3.4 Measuring Radiance

Once the mast is correctly positioned, it is necessary to measure the radiance from a white reference (Spectralon®) panel or use a cosine collector to measure incoming hemispherical irradiance. Following determination of reference spectra or

incoming irradiance, radiance measurements of the target need to be collected at 10° increments in viewing angle. This is easily possible as the viewing zenith (θ) is directly recorded by the digital compass.

The measurement sequence should be as follows: (1) change the viewing zenith (θ) from 0° to 70° at a 10° interval then return to nadir (0°) and remeasure the white panel; (2) change the zenith angle (θ) from 0° to -70° using 10 degree intervals.

Following measurements along this plane, it is necessary to adjust the azimuth angle (φ) in a clockwise direction at 30° intervals and repeating step (1).

4. RESULTS

4.1 *In Situ* Validations

Using field measurements to validate snow albedos retrieved from MODIS data is a feasible and practical method in remote sensing research. In this research, several instruments were used to measure *in situ* surface snow and ice albedos which were further analyzed for validating MODIS albedos.

A three day field campaign conducted on Spirit Lake, IA, from January 29th to 31st provided *in situ* observations that were related to MODIS satellite observations. Most important to validating albedos from the MODIS satellites are those *in situ* albedos retrieved using a Middleton-EP16. As Middlteon-EP16 pyranometer which measured *in situ* albedos during each of the three days during the field campaign, these albedos measured at the same geographic location each can serve as a bench mark for observing the albedo variations during the three days (Fig. 17).

In general, the albedos measured by the EP16 pyrometer on January 29th and 31st are on average 3% higher than the albedos retrieved on January 30th as can be seen in Figure 18. There is also a rapid drop in albedo on January 29th from 13:27 to 14:12 local time resulting from rapidly changing cloud conditions.

On January 29th and 30th, analysis of MOD10A1 images reveals that the Spirit Lake area was cloud-covered so there were no albedo could be retrieved from MODIS during these two days. However, a comparison among MODIS albedo, ETM+ albedo and *in situ* within close dates of the campaign is illustrated in Figure 18. The average *in*

situ albedos from Januray 29th to 31st are 0.74, 0.72, and 0.75, respectively. The MODIS albedos retrieved on 26th 27th , 28th and 31st are 0.75, 0.65, 0.77 and 0.75, respectively. The Landsat ETM+ albedo retrieved on 26th is 0.72. While the EP16 retrieved albedos were found to vary from MODIS retrievals on the same days by only 2.7%, the question remains of how representative was the selected site of the albedo of the entire lake.

To examine spatial variability in albedo over the lake surface, on January 30th, the albedo of twenty-two sites characteristic of the different surface types observed on the lake was examined using LI-COR pyrometers. The surface type observed at each of these sites could be simply classified as ice or snow by examining the photos that were taken at each site. The mean albedo measured at each site further demonstrates the validity of this classification (Fig. 19). Despite some differences in the texture of the snow and ice among the sites, in term of albedo, two general classes emerge. Most sites are snow-covered with LI-COR measured albedos ranging from 75% to 85%. In a few locations, bare ice with albedos approximately 25% lower ranging from 50% to 60% was present. It should be noted that post analysis shows that the albedo from one site (site 6) exceeds 1 so it was excluded from further analysis.

Comparisons of the LI-COR and EP16 albedo measurements made at the same location indicate that the LI-COR and EP16 readings appear to be approximately 10% higher than those of the EP16 (Fig. 20). This suggests that the LI-COR measurements should be corrected in order to better facilitate a comparison of albedos measured with the two instruments.

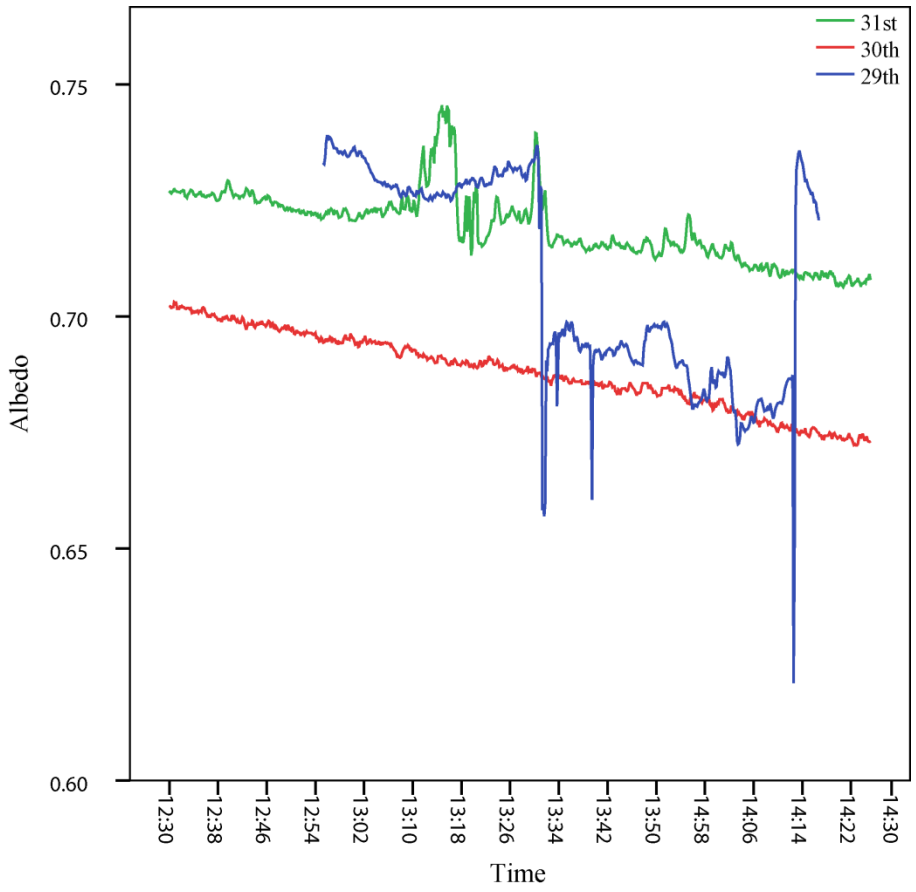

Fig. 17. Comparison of three days' snow albedos retrieved from EP16. They were over both similar time periods and same place.

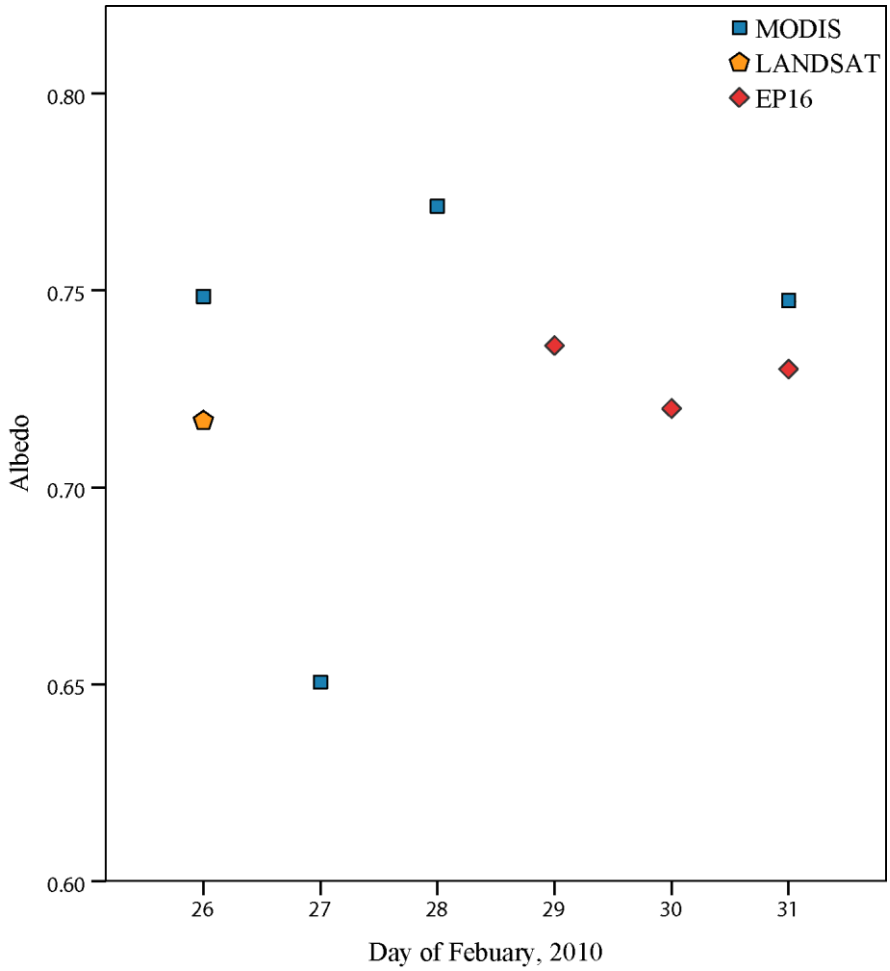

Fig. 18. Comparison of albedos derived from MODIS, ETM+, and EP16 albedometers in time series. The study area was under cloud cover within the week after January 31st, so there is no valuable MODIS10A1 product can be used for comparison.

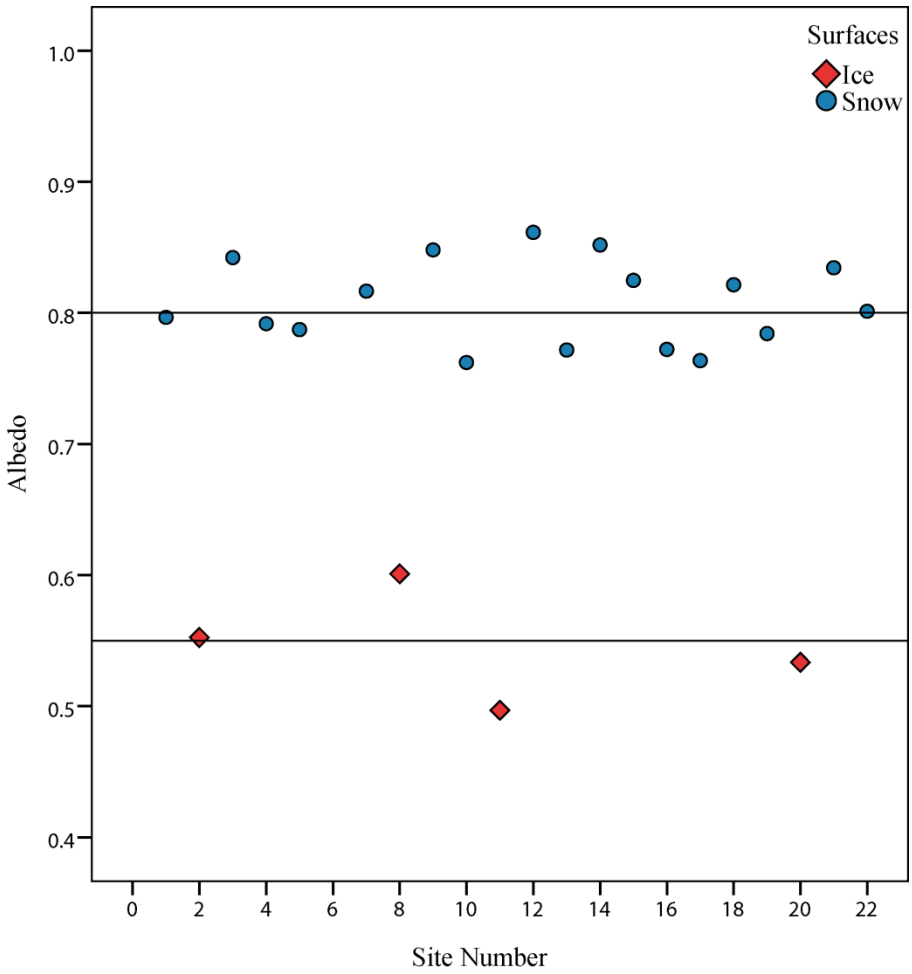

Fig. 19. Albedo variations on January 30th. *In situ* surface albedo measured at twenty-two sites using the LI-COR pyranometers on January 30th.

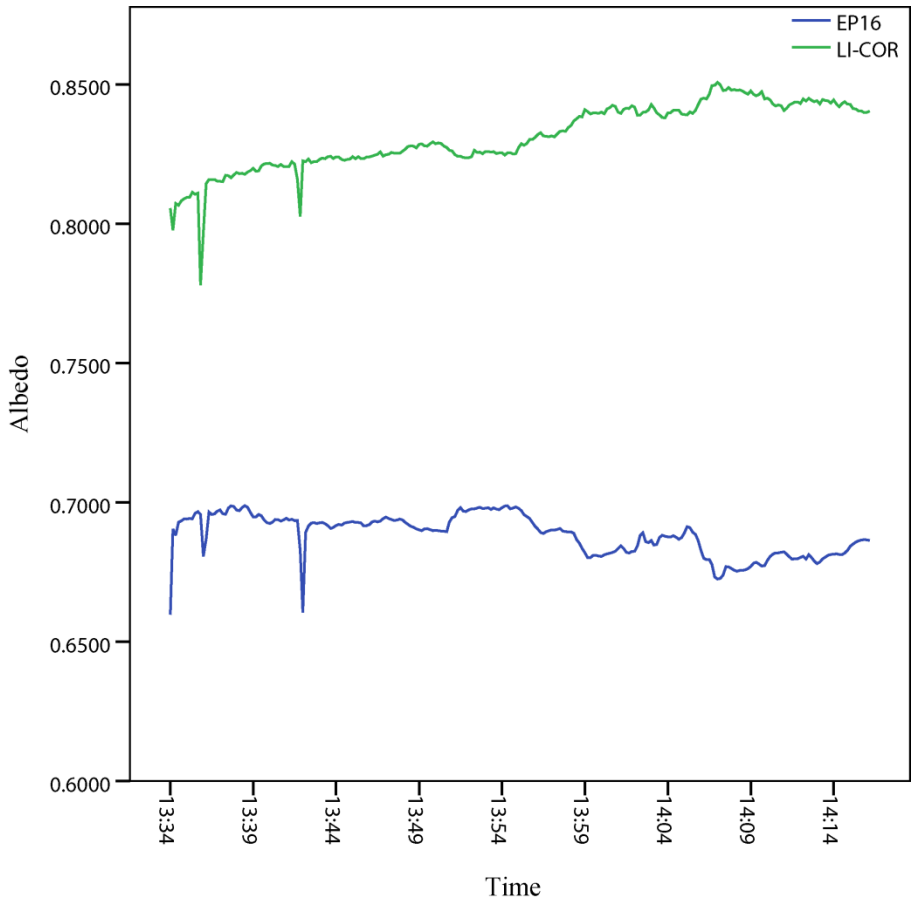

Fig. 20. Albedo discrepancy between two instruments. The albedos retrieved from LI-COR pyrometers and EP16 albedometers on January 29th.

4.2 Spatial Representativeness

It is obvious that over the 1-2 km long transect where albedo measurements were made using *in situ* measurements significant variations in albedo over spatial scales of a few hundred meters even over this relatively uniform roughness surface. Therefore, it appears prudent to further investigate the spatial scales at which snow albedo varies over lakes and other commonly occurring land surface types with varying topography. The results below are for three areas. The first is Spirit Lake which is assumed to be a fairly flat terrain. The second (d1) is a hummocky area associated with the Altamont Moraine Complex while the third (d2) is generally of lower relief and is associated with the Bemis Altamont Moraine Complex which are illustrated in Figure 1 from Chapter 1.

4.2.1 Surface Roughness

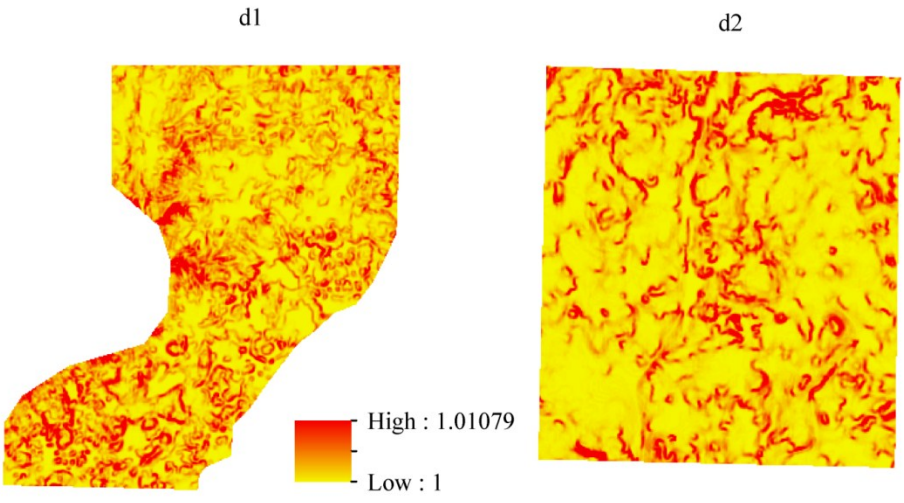

Fig. 21. Surface ratio of site d1 and d2.

The surface roughness maps for two different terrestrial domains were derived from Surface Area and Ratio extension to ArcGIS and is illustrated from Figure 21. This extension can produce a raster in which the surface area values within each cell are divided by the planimetric area within that cell. These derived values could potentially range from 1 to infinity, however, in practice it seldom reaches as high as 3.

The mean surface ratio of d1 is 1.0006 with standard deviation of 0.00075. The average surface ratio of d2 is 1.0002 with standard deviation of 0.00027. Student's t-test indicated that the two mean surface ratios were statistically significantly different at the 0.001 level. This demonstrates that d1 is indeed quantifiably rougher than d2. When the lake is frozen and snow covered, the surface of the lake is nearly flat with topographic variations on the order of 10 cm, so quantitatively the roughness of the lake should approach 1.0. The roughness differences for each domain are potential factor influencing the spatial representativeness of any single albedo measurement made within the domain.

4.2.2 RGB Color Images of Study Areas

Red, green, and blue color composites were constructed from Landsat bands 5, 4 and 2, respectively, and provide a good visual indication of how the different areas appear as snow cover varies from patchy to complete. As can be seen in Figure 22 which illustrates several representative snow cover conditions, the lake is 100% snow covered even when the snow conditions are very patchy for d1 and d2 domains. For these two terrestrial domains as the snow fraction increases, the cultural infrastructure becomes more obvious.

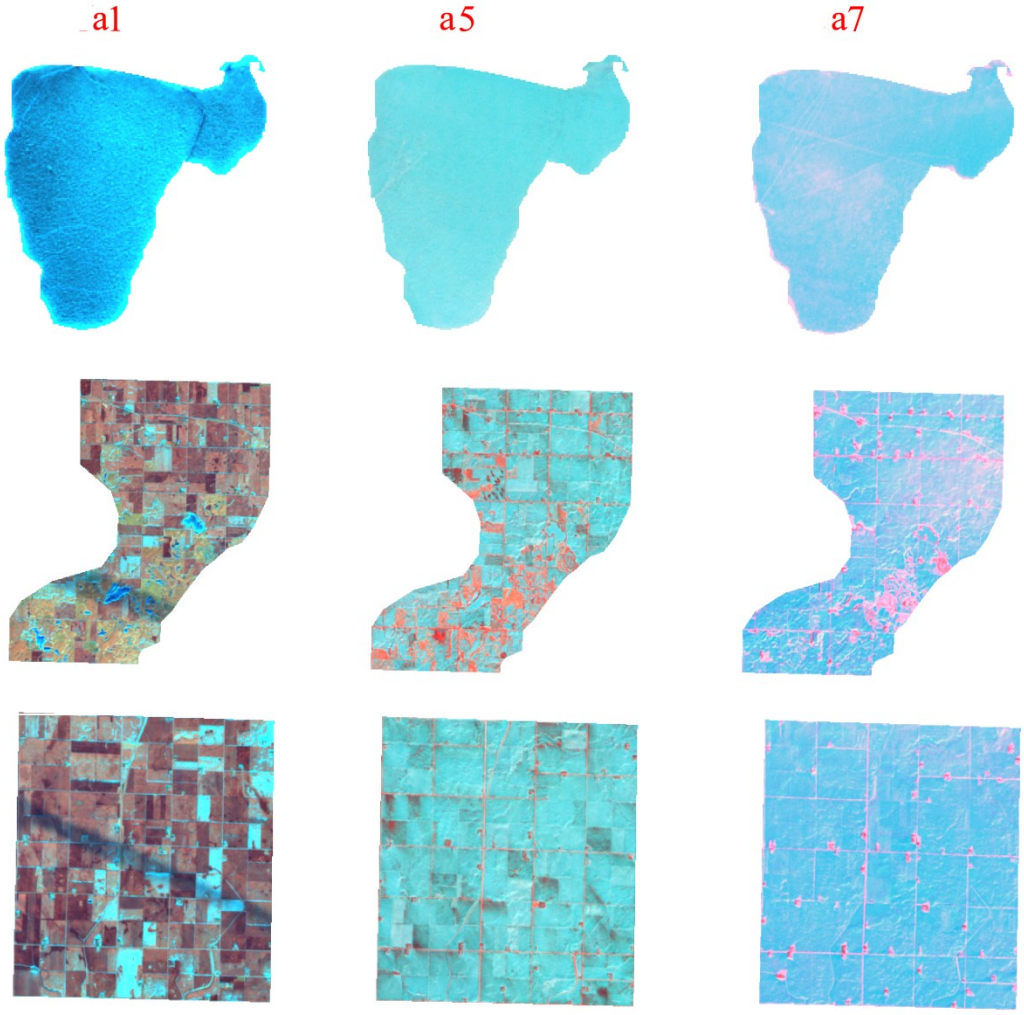

Fig. 22. RGB (5,4,2) color composite maps of three scenes for study areas.

4.2.3 Snow Albedo

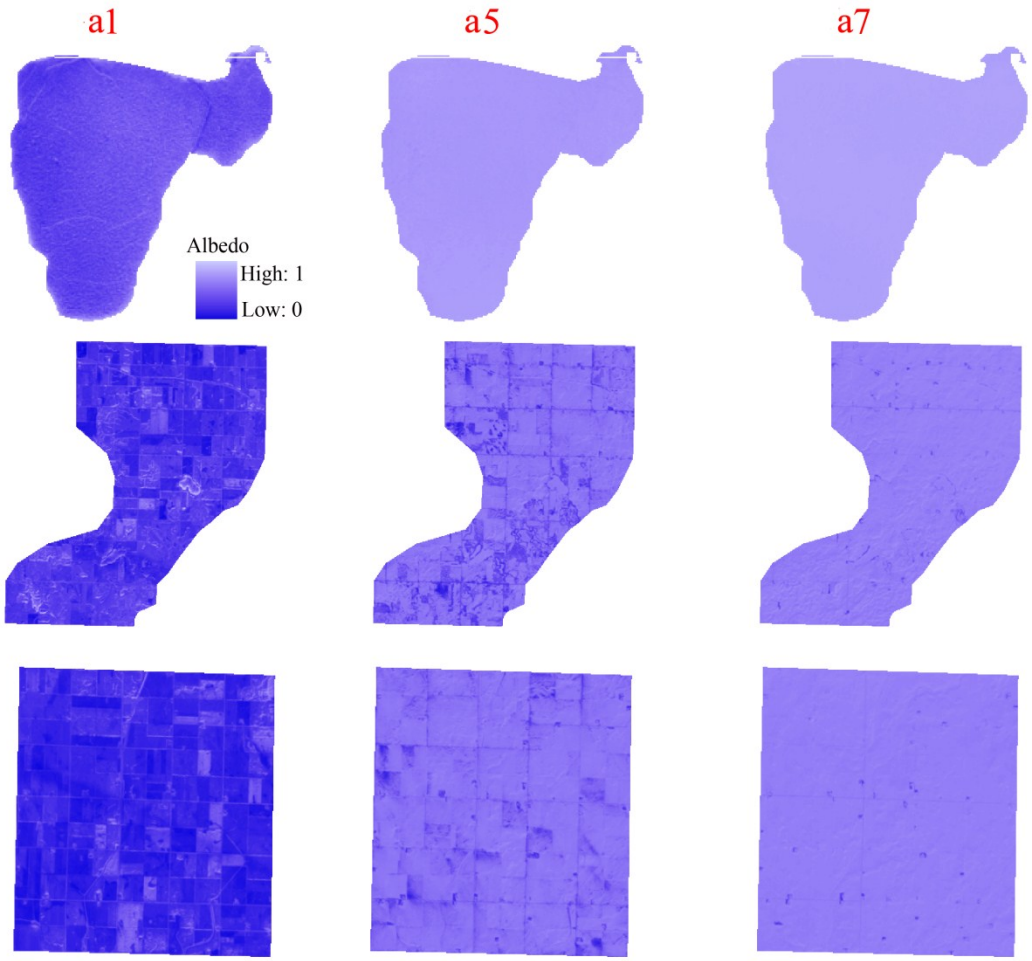

Fig. 23. The albedo maps of three scenes for study areas.

Selected Landsat-derived albedo images for representative snow cover conditions are illustrated in Figure 23. From these images, it is clear that there is little albedo variation across the lake, with the possible exception of when snow cover is very patchy (a1). Spatial variability in albedo is higher for the two terrestrial domains. In general, as the snow fraction increases the overall albedo for each study site increases as can be seen in the lighter colors when snow cover is more extensive (a5 and a7).

4.2.4 Binary Snow Mapping

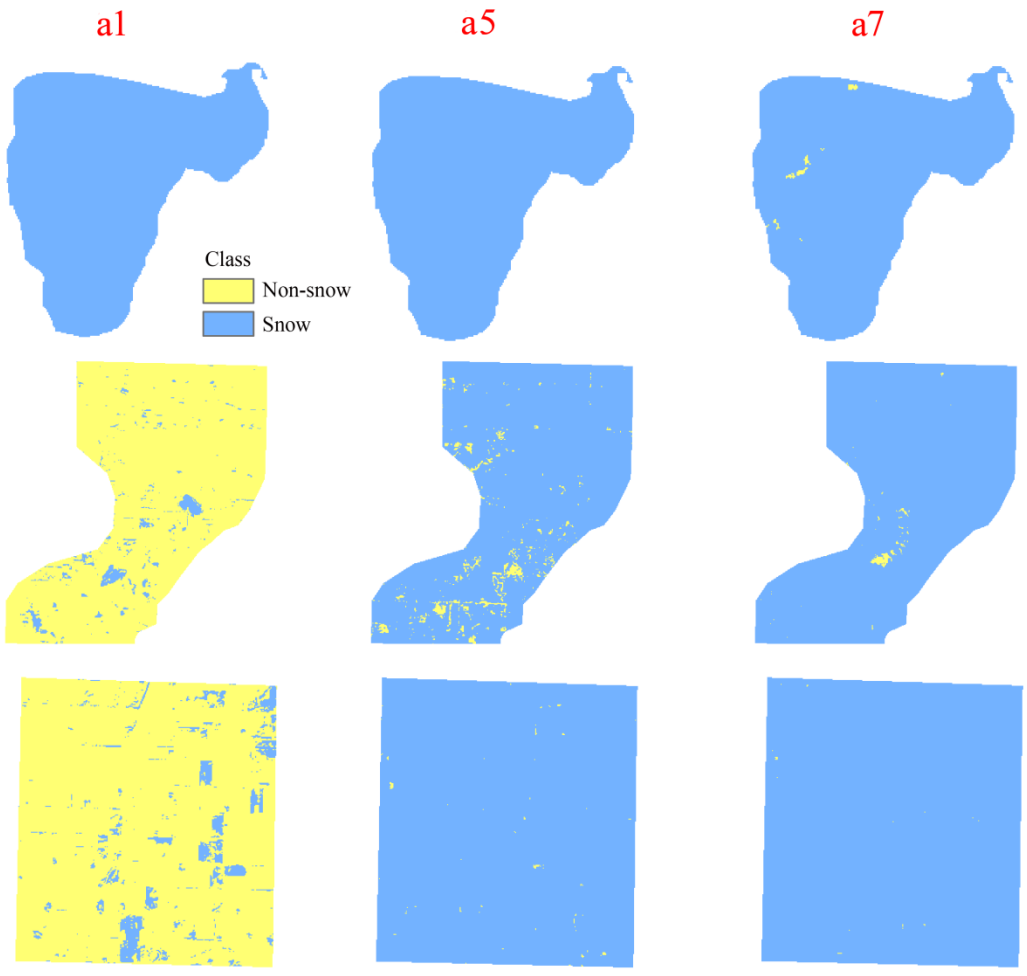

Fig. 24. The binary snow maps of three scenes for study areas.

Landscape metrics were derived from the binary snow maps which are illustrated in Figure 24. Each pixel in these images was classified as snow or non-snow. For d1 and d2 in the most patchy scene a1, the dominant land cover is non-snow (yellow). As the snow fraction increases, snow cover (blue) increases.

4.2.5 Semivariogram Analysis

Using the Landsat-derived albedo maps (Fig. 23), the range distance was determined from each of the modeled semivariograms (Fig. 25, Fig. 26. and Fig. 27). These range distances provide an indication of the spatial autocorrelation lengths of snow albedo as at distances larger than the range, albedos can be considered uncorrelated. To further examine what factors can influence the variation of these ranges, several ancillary variables were analyzed, including surface roughness (Fig. 28, Fig. 29), snow fraction (Fig.30, Fig.31), Mean Shape Index (Fig. 32) and Area Weighted Shape Index (Fig. 33).

For most snow conditions, the albedo range distance exceeded 250 meters, which suggests that an *in situ* albedo measurement is characteristic of areas approaching the size of low resolution satellites such as MODIS. In general range sizes for the homogeneous lake are larger than the two rougher domains (Fig. 28). For the lake, the range size increases when snow fraction increases. However, this did not occur in terrestrial domains (i.e. d1 and d2). In these two domains, the semivariogram range sizes of snow albedo of domains d1 and d2 tended to decrease as the percentage of snow cover in the studied domains increased (Fig. 29).

For d1 and d2, the relationship between snow ranges and snow fraction was further examined (Fig. 30). When the snow fraction exceeded 90 percent, the range distance significantly decreases as the snow fraction increases (Fig. 31).

Similarly, the relationship between the albedo range size and surface roughness as characterized by the two shape indexes was examined and the results are illustrated in Figure 32 and Figure 33. The correlation coefficient between ranges and MSI was relatively weak at 0.275 while the correlation coefficient between the ranges distance and the AWMSI was somewhat stronger at 0.416.

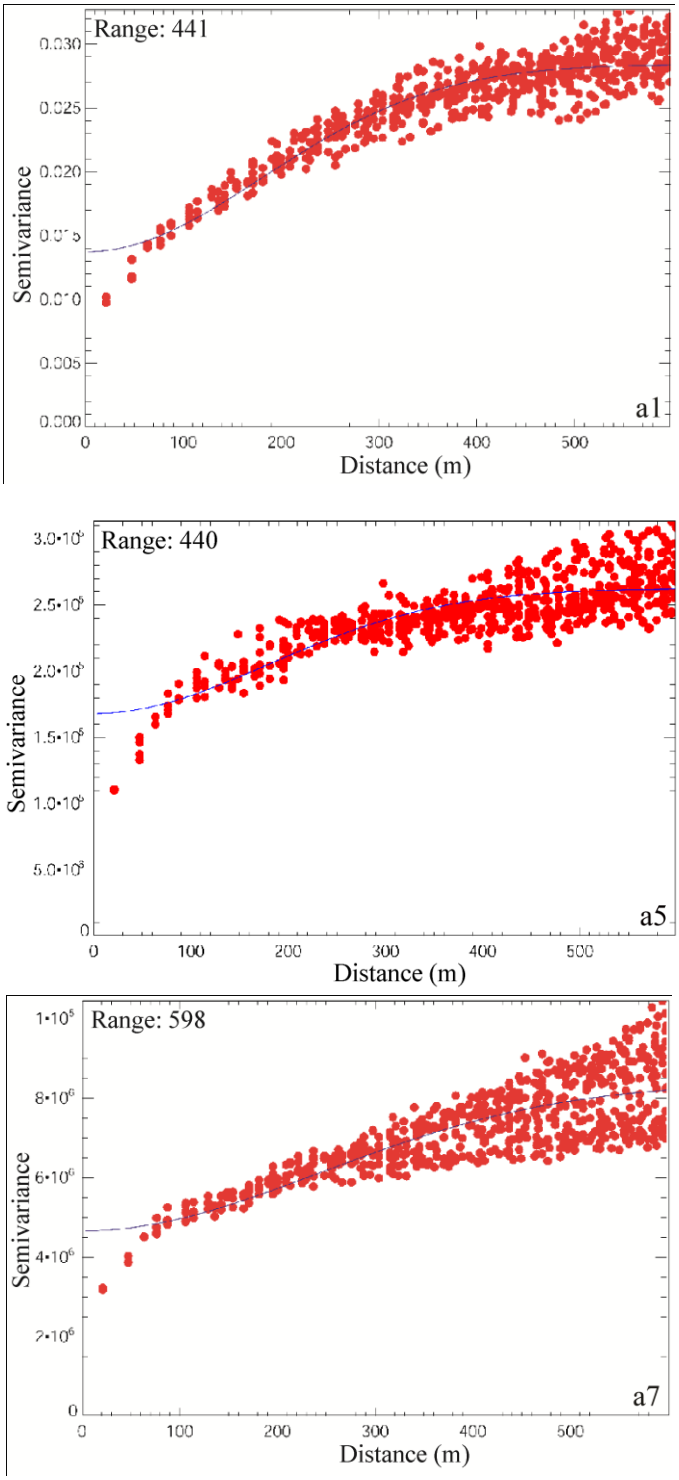

Fig. 25. Semivariograms of albedo derived from Big Spirit Lake. From top to bottom these are the semivariograms of scenes a1, a5, and a7. The range size (m) from the fitted semivariogram is also shown.

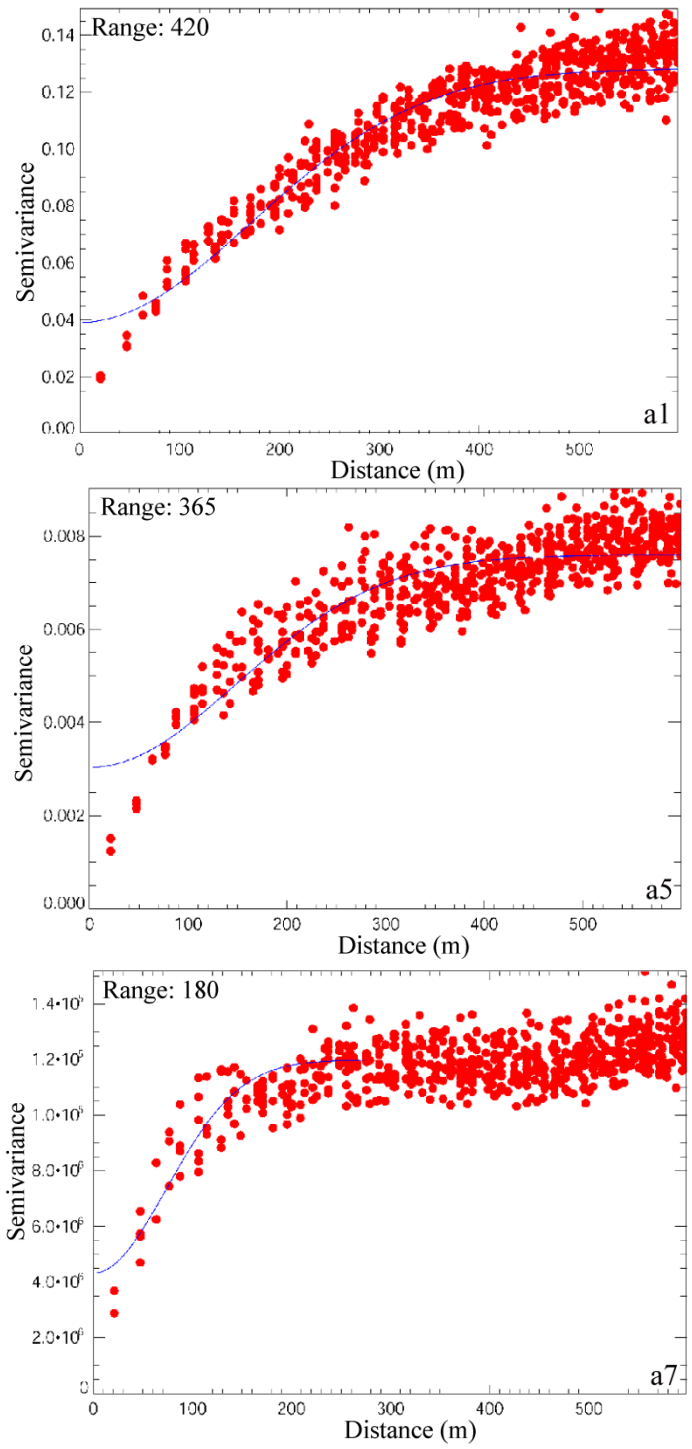

Fig. 26. Semivariograms of albedo derived from d1. From top to bottom these are the semivariograms of scenes a1, a5, and a7.

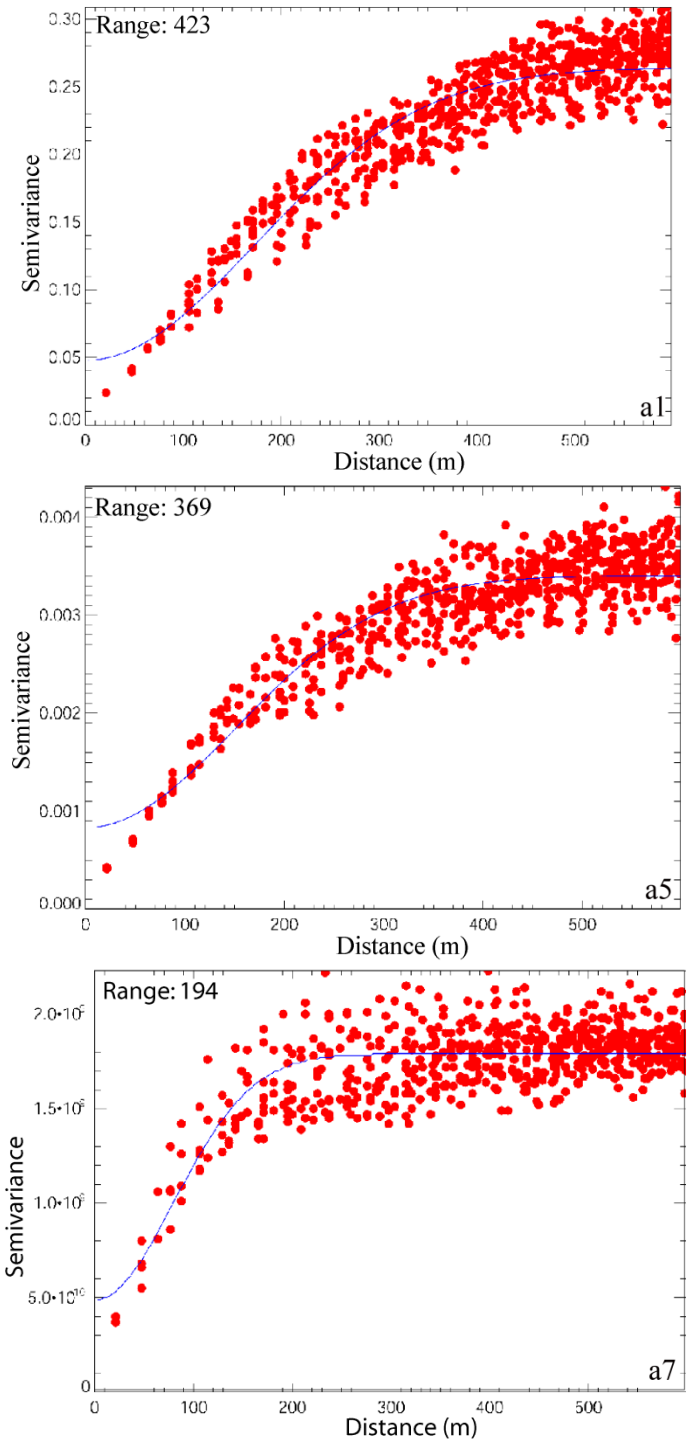

Fig. 27. Semivariograms of albedo derived from d2. From top to bottom these are the semivariograms of scenes a1, a5, and a7.

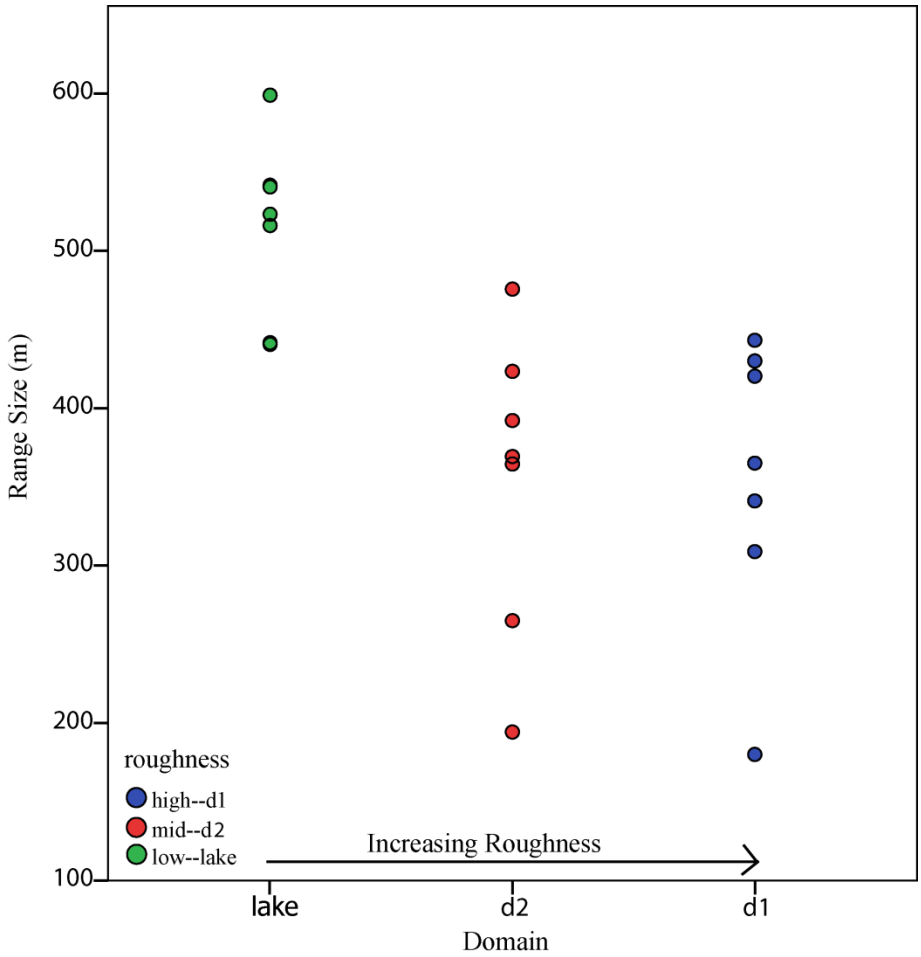

Fig. 28. Semivariogram ranges for different domains. The topography of d1 is rougher than d2 while the topography of d2 is rougher than that of Big Spirit Lake.

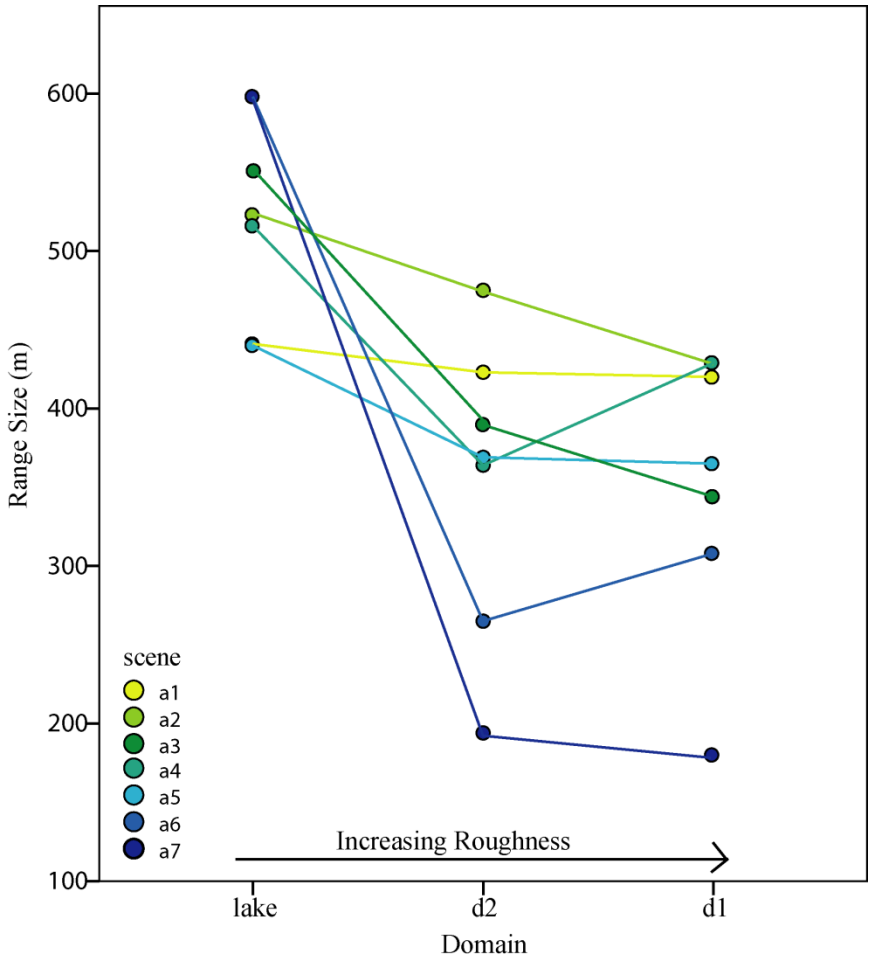

Fig. 29. Semivariogram ranges for different scenes. The different colors indicate the semivariogram range sizes derived for each of the seven studied Landsat scenes.

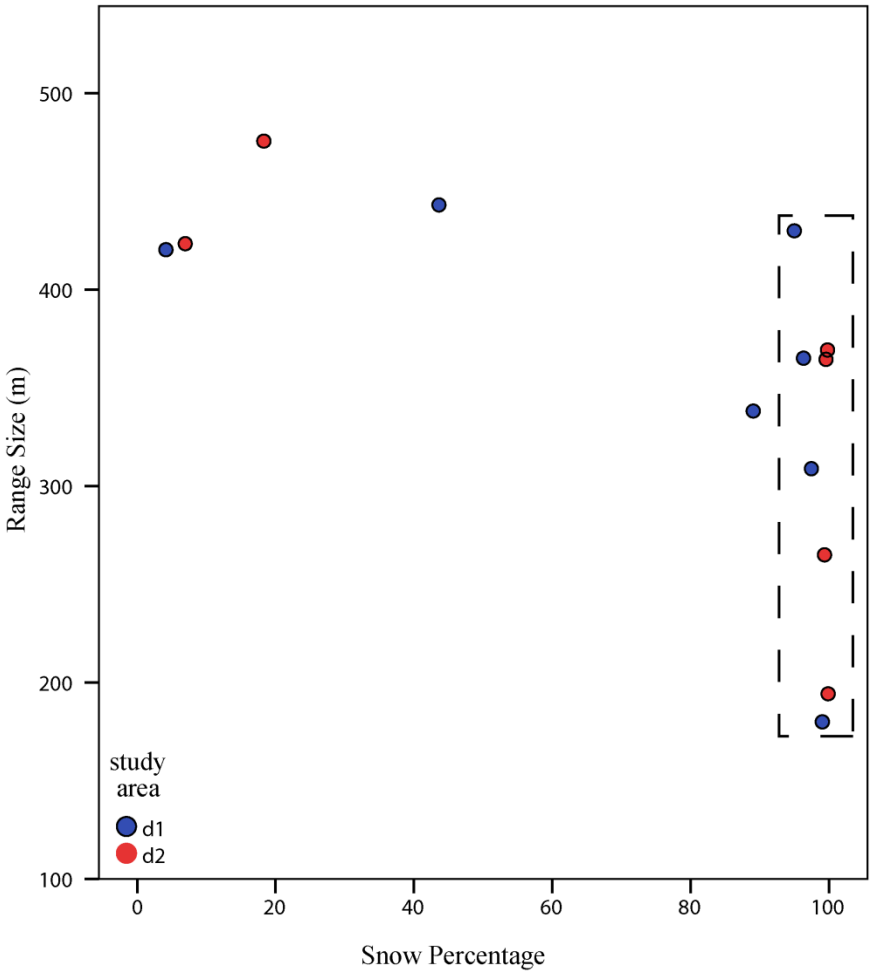

Fig. 30. The relationship between ranges and snow fraction of study areas. The dashed box indicates the range of snow cover percentages illustrated in Figure 28.

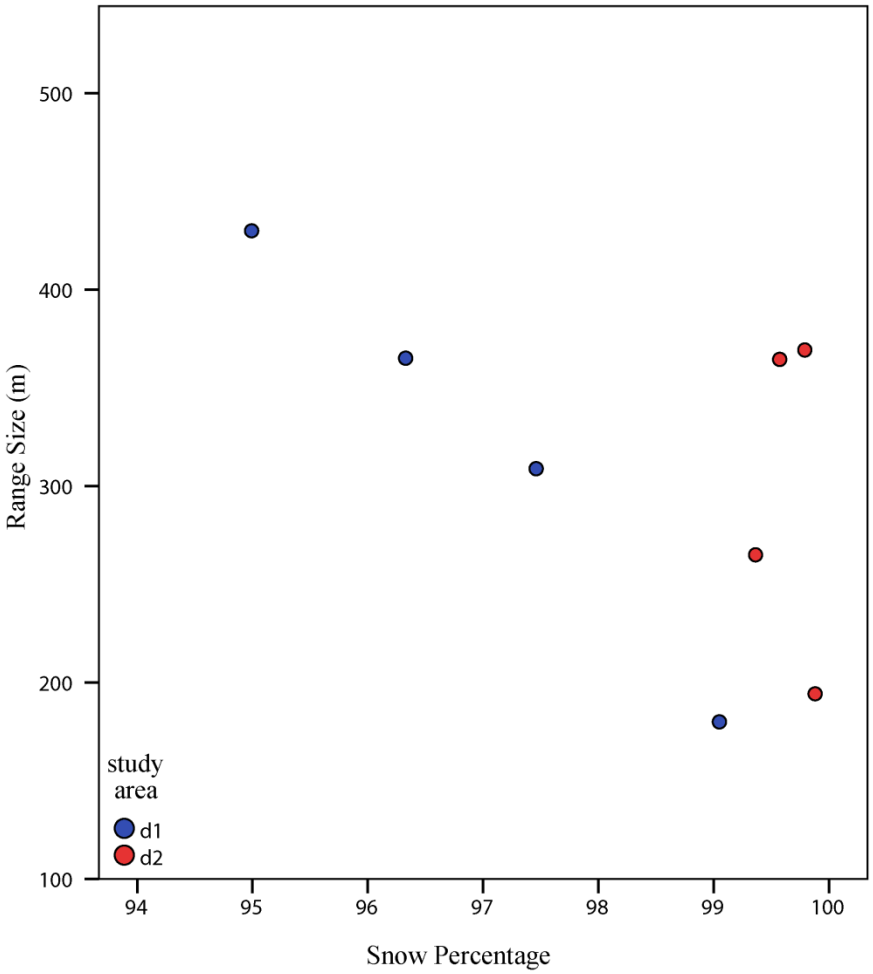

Fig. 31. The relationship between ranges and snow fraction of study areas for snow-cover fractions approaching 100 percent. This figure represents the snow covered fractions in the dashed box shown in Fig. 30.

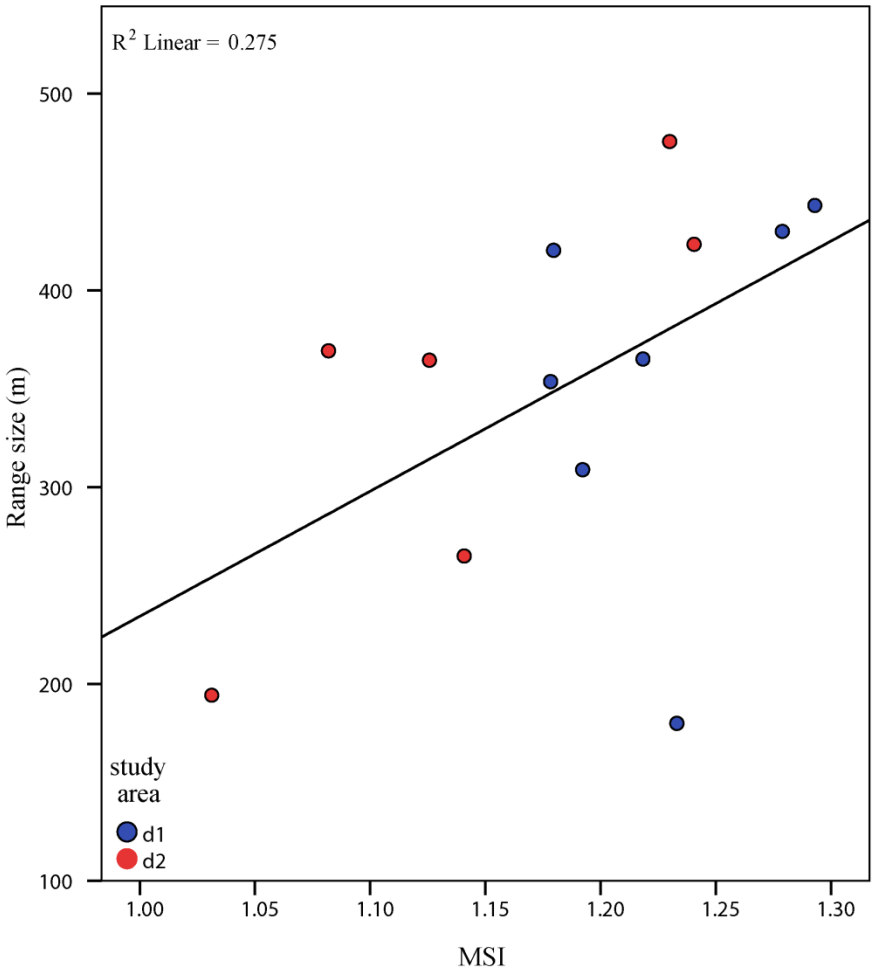

Fig. 32. The correlations between ranges and mean shape index (MSI).

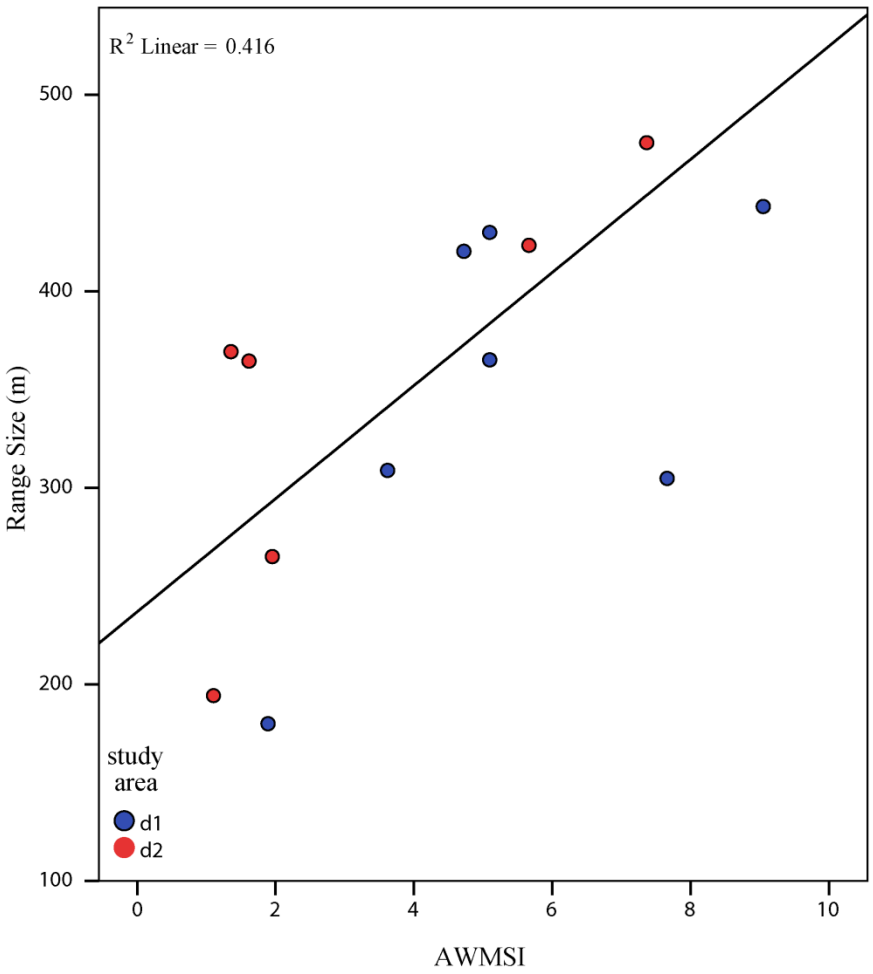

Fig. 33. The correlations between ranges and area weighted mean shape index (AWMSI).

4.3 Station Validations

The results presented previously suggest that for relatively homogeneous areas, a single *in situ* albedo measurement can be considered fairly representative of a MODIS pixel. Therefore it seems reasonably to use albedos measured at carefully selected measurement sites to validate the MODIS daily albedos during the snow season. Therefore, *in situ* albedos measured at the Fort Peck, Montana, SUFRAD site and the Barrow, Alaska, ARM site were compared to MOD10A1 snow albedos.

The snow season was determined as follows. Station albedos were first retrieved and examined. There are two criteria for determining the snow melting dates. First, snow albedo is normally higher than 0.6, and after snow melt the albedo drops to much lower values. Also, before melting, there should be a period which is long enough to build and maintain a snowpack. Using these two criteria, a date window from March 30th to June 15th was selected for Barrow during 2008 and 2009 to capture the end of the snow season. For Fort Peck, however, there is no sufficient snow in the beginning of 2008, so alternatively, a date window from January 19th to April 9th for 2009 and 2010 was examined.

For 2008 Barrow data, twenty-one scenes out of seventy-seven MODIS scenes have snow albedo values that fall in the theoretically-expected range of 0 to 100. The relationship between these MODIS and *in situ* albedos is illustrated in Fig. 34. The correlation coefficient is 0.785. For the 2009 Barrow data, twenty scenes out of seventy-seven were useable. The relationship between MODIS and *in situ* albedo is shown in Fig. 35. The correlation coefficient is 0.725.

For the 2009 Fort Peck MODIS data, twenty-three out of eighty scenes were sufficiently cloud-free to use. The relationship between MODIS and *in situ* is shown in Fig. 36. The correlation coefficient is as low as 0.404. For the data Fort Peck in 2010, only eight scenes out of seventy-eight scenes were usable and the correlation between MODIS and the *in situ* observations is higher at 0.663 (Fig. 37).

From all the valid datasets, there are seventy-two total scenes that can be used to examine the correlation between the *in situ* and MODIS-derived alebdos (Fig. 38) which

was found to be 0.583. The root mean square error (RMSE) of each comparison is summarized in Table 7.

Table 7. The RMSE and R^2 of albedo validations for each data set.

Data set	R^2	RMSE
Barrow 2008	0.785	7.1%
Barrow 2009	0.725	6.7%
Fort Peck 2009	0.404	8.6%
Fort Peck 2010	0.663	5.1%
Overall	0.583	8.4%

The relationship between *in situ* temperature and *in situ* albedo during the snow season is illustrated by plotting temperate and snow albedos together in Figures 39, 40, 41 and 42. In addition, the available MODIS albedos are also plotted in these figures as a comparison between *in situ* albedo measurements.

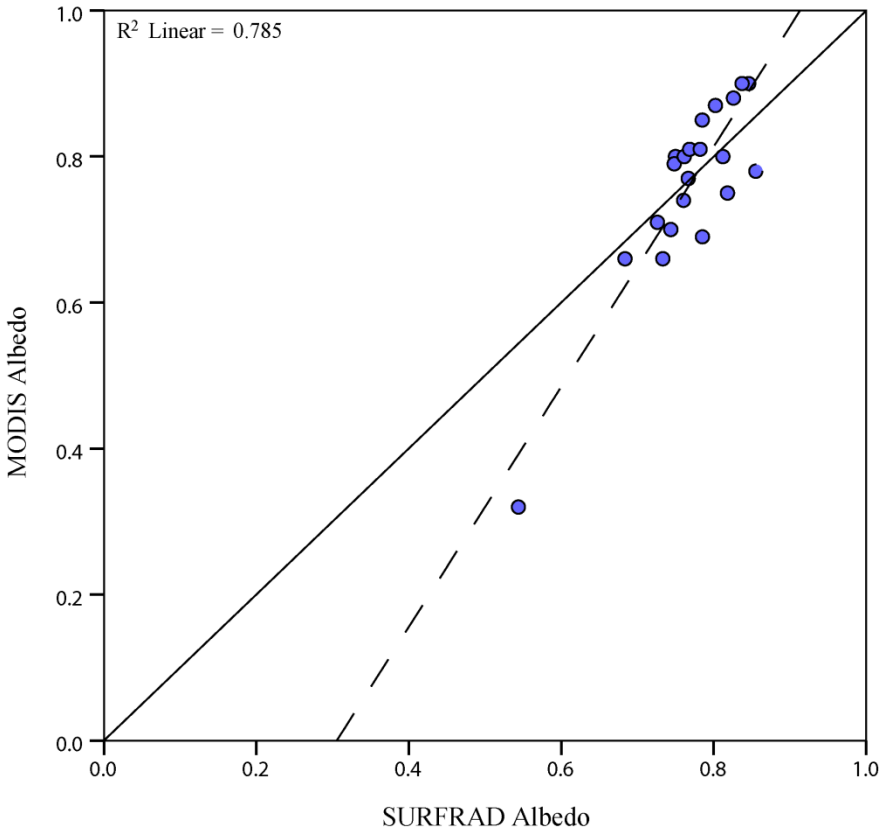

Fig. 34. The albedo correlation between MODIS and Barrow station in 2008.

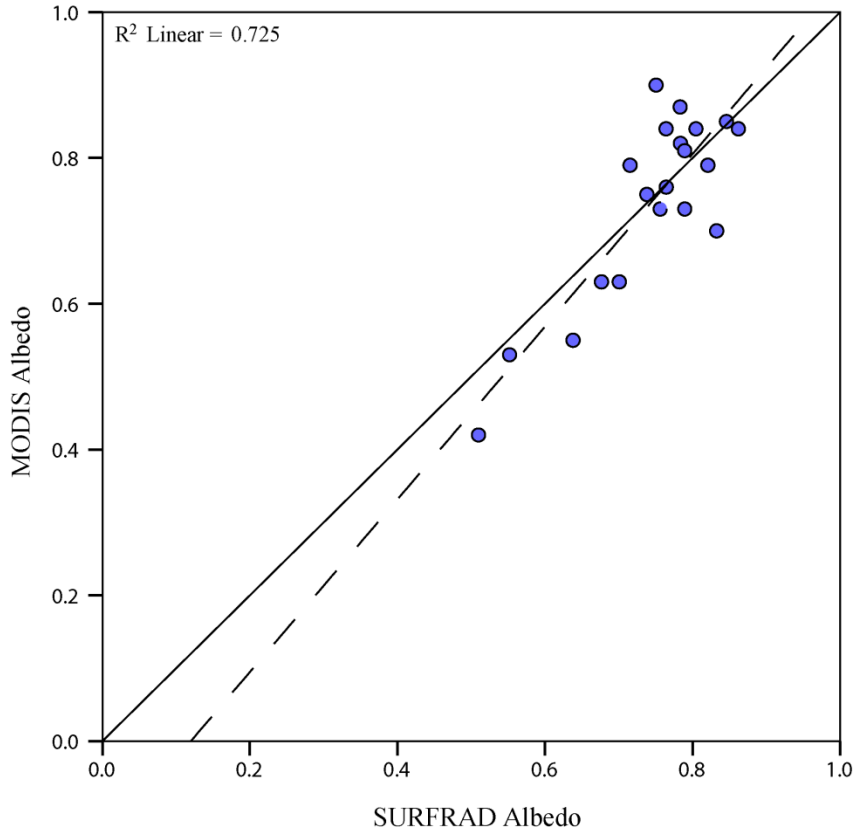

Fig. 35. The albedo correlation between MODIS and Barrow station in 2009.

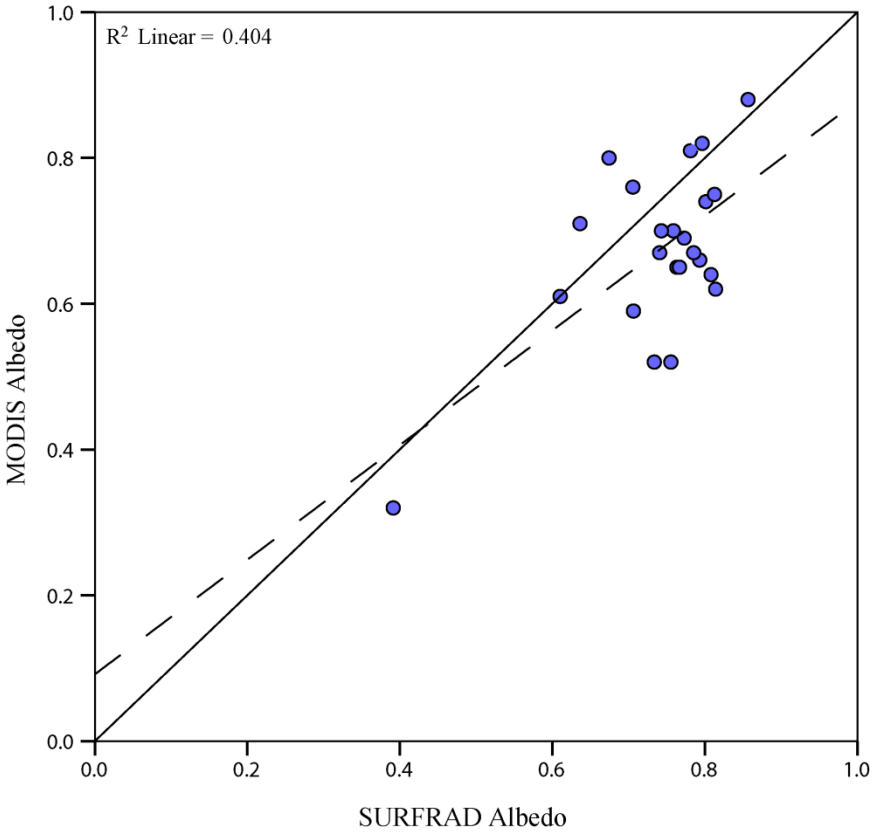

Fig. 36. The albedo correlations between MODIS and Fort Peck station in 2009.

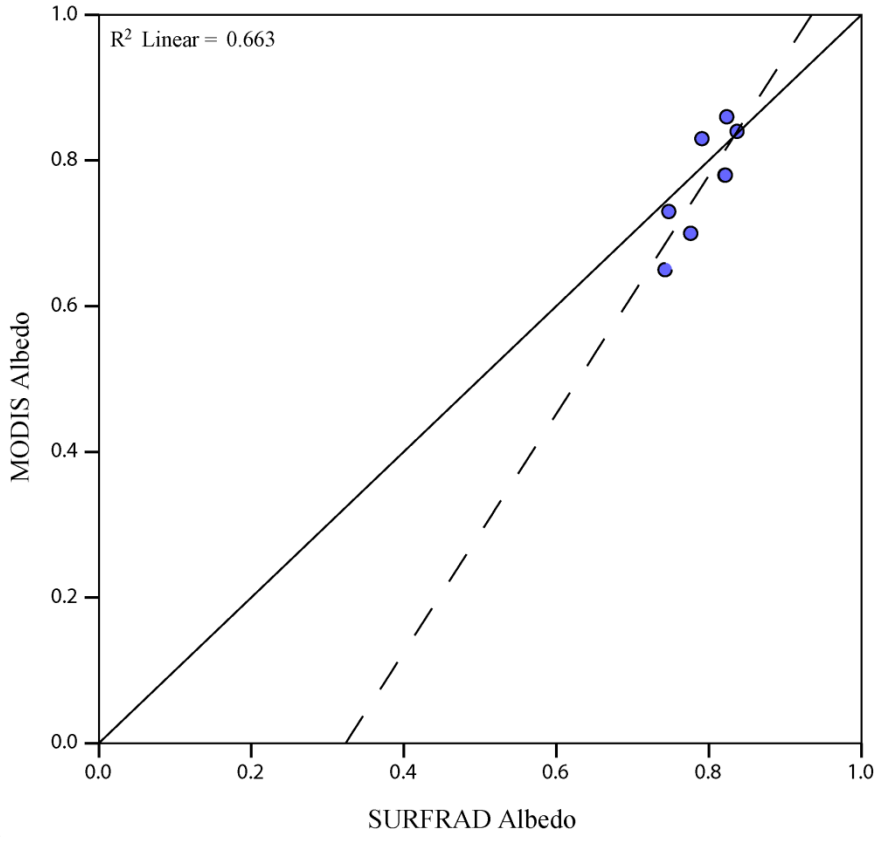

Fig. 37. The albedo correlations between MODIS and Fort Peck station in 2010.

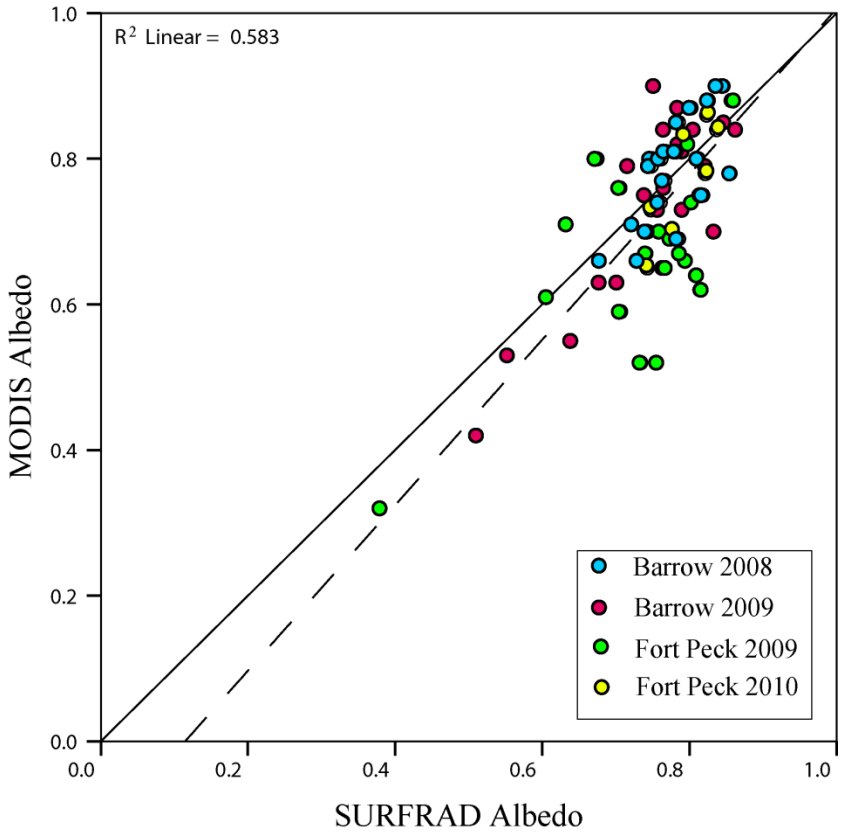

Fig. 38. The albedo correlations between MODIS and the four datasets.

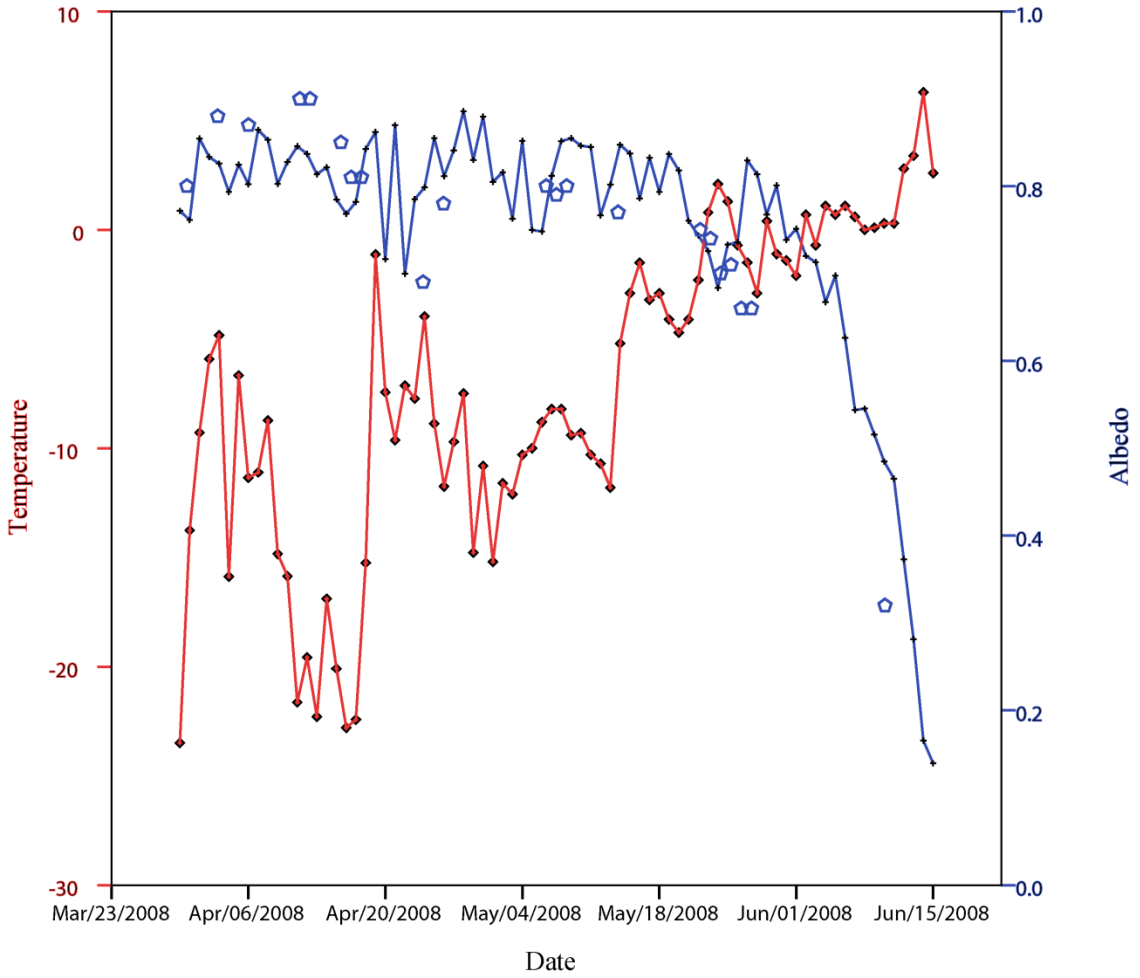

Fig. 39. Temperature and albedo trend of Barrow 2008. The blue line is the station albedos. The red line is the temperature. The pentagon is the MODIS albedo.

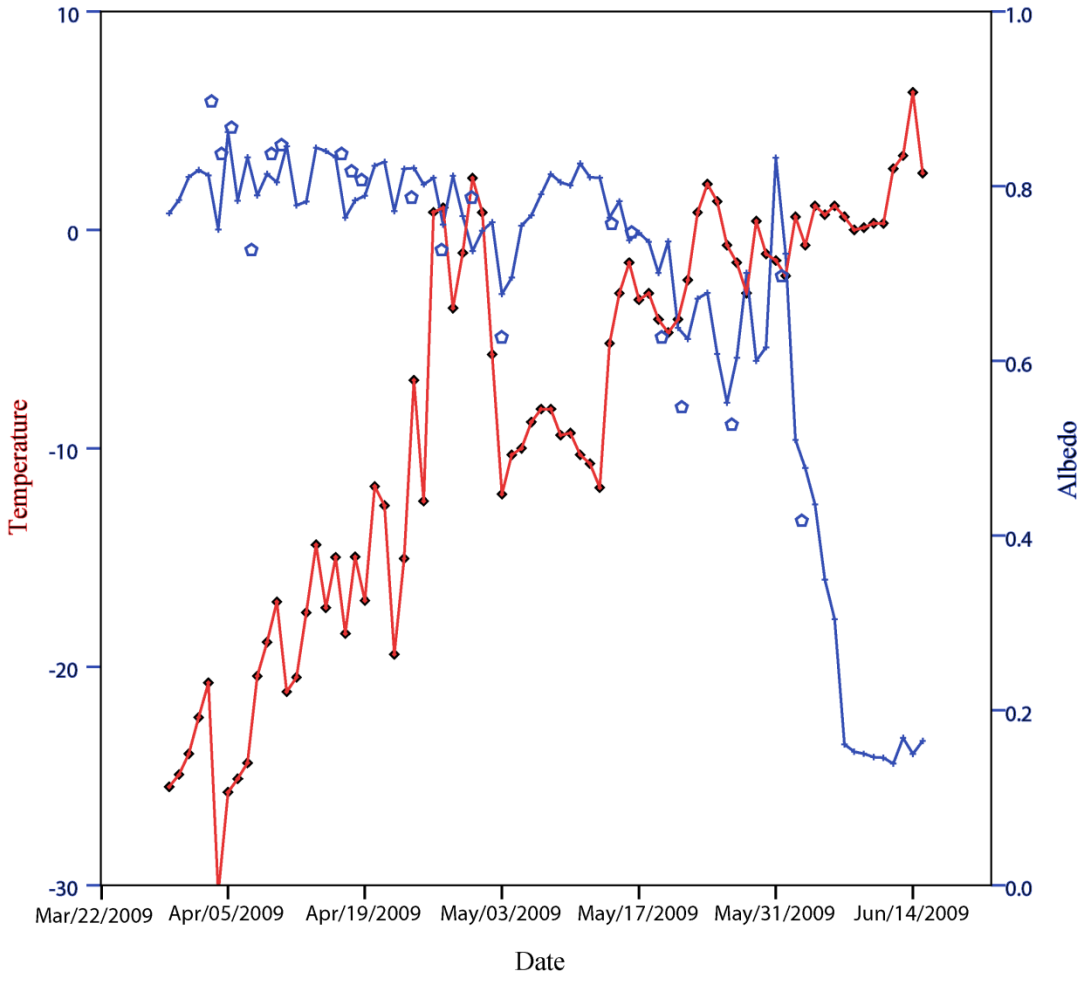

Fig. 40. Temperature and albedo trend of Barrow 2009. The blue line is the station albedos. The red line is the temperature. The pentagon is the MODIS albedo.

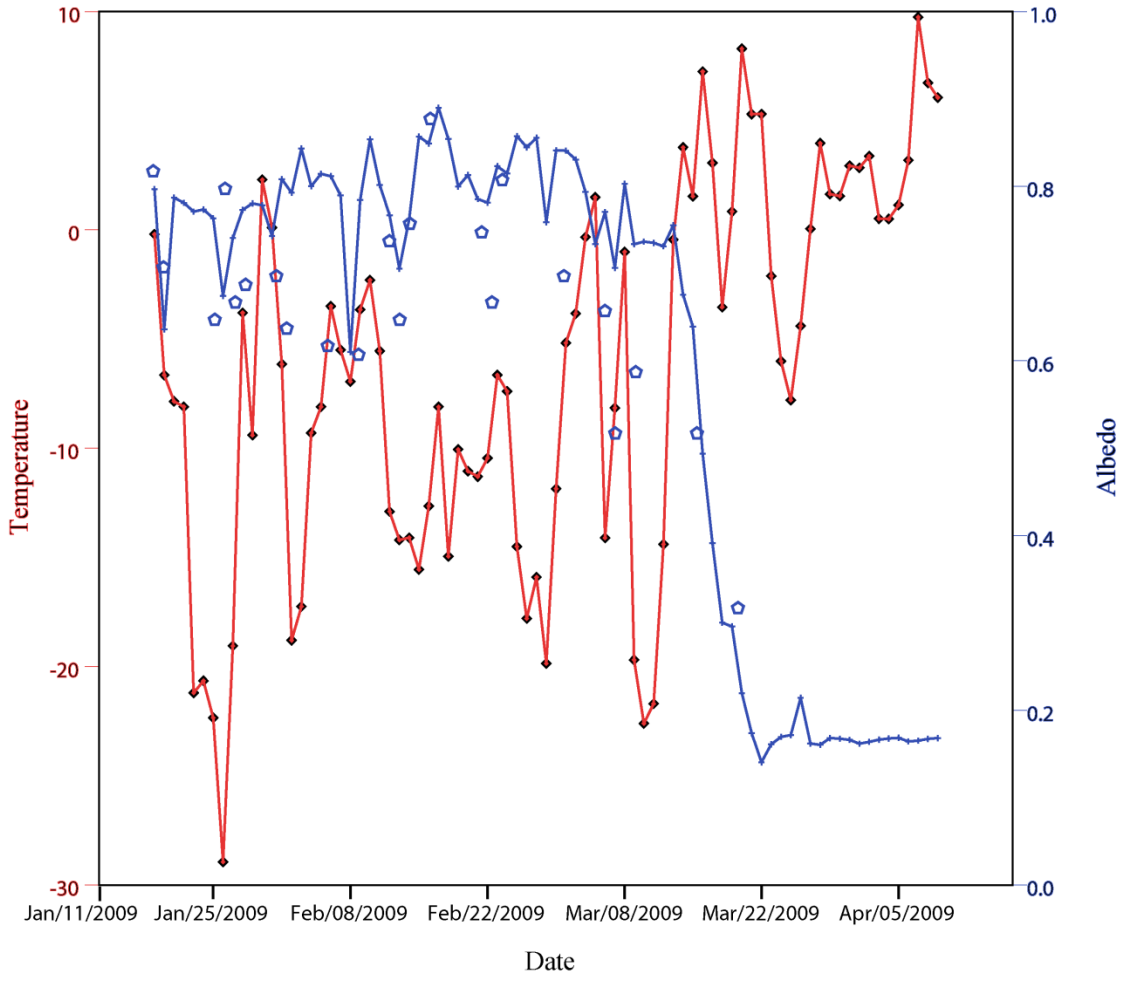

Fig. 41. Temperature and albedo trend of Fort Peck 2009. The blue line is the station albedos. The red line is the temperature. The pentagon is the MODIS albedo.

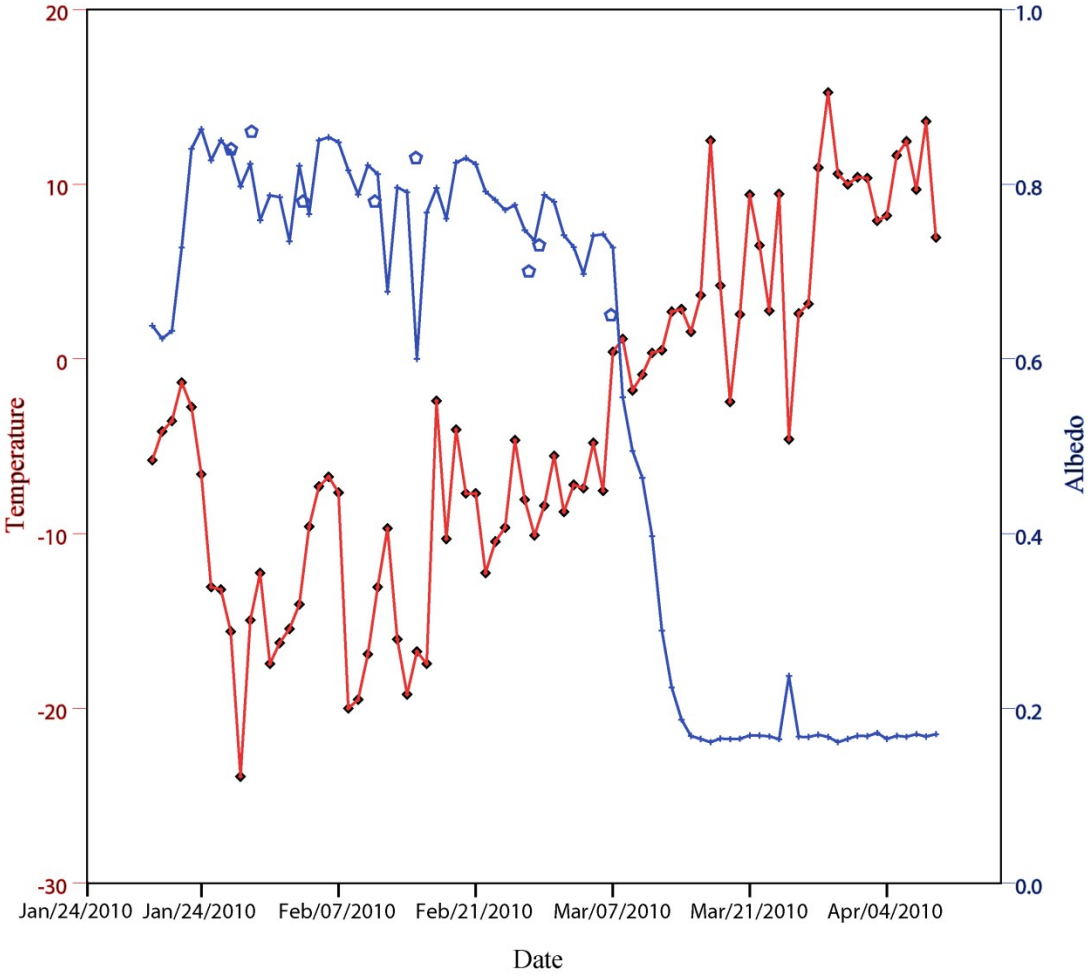

Fig. 42. Temperature and albedo trend of Fort Peck 2010. The blue line is the station albedos. The red line is the temperature. The pentagon is the MODIS albedo.

5. DISCUSSION

5.1 *In Situ* Validations Analysis

Overall, good agreement was found between the MODIS albedo and *in situ* albedo on January 31st (Fig. 18) over Big Spirit Lake with the two albedos differing by only 2.7%. This frozen lake covered with snow is very flat and homogeneous land cover. However, even its homogeneously surface, large variations in albedo were still found to exist that can affect our ability to use these surfaces to validate satellite retrievals of snow albedo (Fig. 19).

This research highlights another problem in validating snow albedos and that relates to the possibility of significantly different albedos retrieved from different instruments. Inexpensive LI-COR instruments only measure albedo in a narrow range of wavelengths (300 to 1100 nm) while more expensive thermopile based instruments such as the Middleton EP16 measure over a much larger spectrum (300 nm to 2800 nm). In addition, snow's spectral albedo drops significantly from the infrared band (i.e. 1000 nm) because snow particle absorbs more energy in infrared spectrum than visible spectrum (Liang, 2000). Taking these facts into account may explain why the shortwave albedo retrieved from LI-COR is normally 3% higher than the albedo retrieved from EP16 when over the same surfaces (Liang, 2002). Similarly magnitude differences were noted between the EP16 and the LI-COR instruments used in this study by Klein (2003). However, analysis of the 2010 Iowa field albedos acquired over Big Spirit Lake shows that even in the same condition (i.e. time, surface types, sun illumination etc.), the

albedo retrieved from LI-COR is approximately 10% higher than the one retrieved from EP16 (Fig. 20). The reason for this discrepancy is unclear, but there are several potential issues that could have led to this observed difference, including leveling and calibration problems.

Changing snow conditions can also hinder the ability to validate satellite retrievals using *in situ* measurements. The analysis of albedo retrieved from EP16 albedometers (Fig. 17) shows that in general, the albedos on the 29th and 31st are both higher than the albedos retrieved on the 30th. This difference was caused by two snow falls in the late afternoons on January 28th and 30th which would be expected to increase albedo. Also, as seen in Figure 14, at the site in the center of Spirit Lake, the measured albedo dropped over the course of each day. This suggests that the albedo changes along with changes in sun's elevation as a response to the highly non-lambertian reflection from the surface. In addition, there is a significant drop of albedo on the 29th between 13:30 and 14:15 caused cloud shadowing the sun which can lead to the low albedo.

The Landsat albedo aggregated to the size of the MODIS pixel using the method of Liang et al. (2002) showed a strong similarity between Landsat and MODIS-derived albedos. This also suggests that the current MODIS snow albedo product provides fairly accurately retrieved albedos over this homogeneous snow-covered lake during our study period.

5.2 Spatial Representativeness Analysis

While the *in situ* measurements studied here compare well to the MODIS snow albedo retrievals, they do not address the question of whether or not a snow albedo

measurement made at a particular location can be considered representative of an entire MODIS pixel – even over a homogeneous site like Big Spirit Lake. Therefore additional analysis was undertaken to investigate this as well as to investigate how the representativeness of an *in situ* measurement could be expected to vary as snow fraction increases.

Ideally, as the snow fraction increases, an *in situ* observation should become representative of a larger area. In geostatistics, this phenomenon should be captured by an increasing range size in the semivariogram as the surface becomes more homogeneous. This assumption was found on the frozen lake (Fig. 28). However, somewhat paradoxically, in the two terrestrial domains a contradictory result – decreasing ranges as the snow fraction increases was found as is illustrated in Figure 29.

In the terrestrial domains d1 and d2, as snow fraction increases, the ranges were found to decrease (Fig. 30), especially when the snow fraction is over 94% (Fig. 31). This is because when under low snow coverage, the albedos of partially snow-covered agricultural fields and adjacent roads and farmsteads were fairly similar. However, as the snow fraction increased, the spatial patterns in albedo became more complex as the albedo contrasts between high albedo snow-covered fields and lower albedo cleared roads and farmsteads (cleared and containing more trees) becomes greater.

FRAGSTATS is widely used in the field of ecology to quantify landscape structures. When examining the relationship between landscape metrics and ranges, many parameters were examined by the aid of FRAGSTATS, including shape index (SI), core area index (CAI), edge contrast index (ECI), Nearest Neighbor Distance

(NND), Proximity Index (PI) etc. However, only two relationships were found among these metrics: the mean shape area index (MSI) and area weighted mean shape index (AWMSI) (Fig. 32 and Fig. 33). The correlation coefficient between ranges and MSI was 0.275 while the correlation coefficient between the ranges distance and the AWMSI was 0.416. This suggests that snow's spatial distribution is a critical parameter influencing the representativeness of one *in situ* measurement.

5.3 Station Validations Analysis

This study also employed two additional sites to investigate the accuracy of the MODIS snow albedo product in comparison to *in situ* observations. Overall, adequate agreement was found between MODIS snow albedos and observations made at the Fort Peck SURFRAD Site in Montana and the ARM site at Barrow, Alaska.

The correlation coefficient of all the available MODIS observations at these two sites is 0.583 (Fig. 38) and the associated Root Mean Square Error (RMSE) between the two albedo estimates is 8% , which suggests that the MOD10A1 product works well to estimate the snow albedo over these two areas. However, the RMSE is a little higher than the validations conducted in Greenland Ice Sheet by Stroeve et al, which is 7% (2006). One possible explanation for the greater difference is that the Greenland Ice Sheet is a more homogeneous land surface than either of the two SURFRAD station sites examined. Therefore the *in situ* albedo measured in Greenland would be expected to be more representative of a MODIS pixel and a lower RMSE would be expected. In addition, the MODIS product underestimates the snow albedos in the year of 2009 at

Fort Peck (Fig. 41), but works well in other three datasets. This underestimation could be resulted by the different snow conditions including snow depth.

In order to investigate this underestimation, snow depth data were retrieved and examined during the two studied snow seasons both at Barrow and Fort Peck. There was adequate snow depth with most depths above 10 cm at Barrow (Fig. 43) during both 2008 and 2009. At Fort Peck, there was sufficient snow in 2010 and most snow depths again being above 10 cm. However, snow depths were much lower at Fort Peck in 2009 (Fig. 43). The lower snow depths in 2009 at Fort Peck is one reason that leads to the MODIS albedos' underestimation at this time.

When plotting the difference between *in situ* and MODIS albedo with snow depth, the underestimation in snow albedo from MODIS that tends to accompany thinner snow packs is apparent (Fig. 44). In Figure 44, when the snow depth is under 10 cm, MODIS tends to underestimate snow albedo to the *in situ* measurements. In addition, most of these underestimated points belong to the 2009 Fort Peck data set.

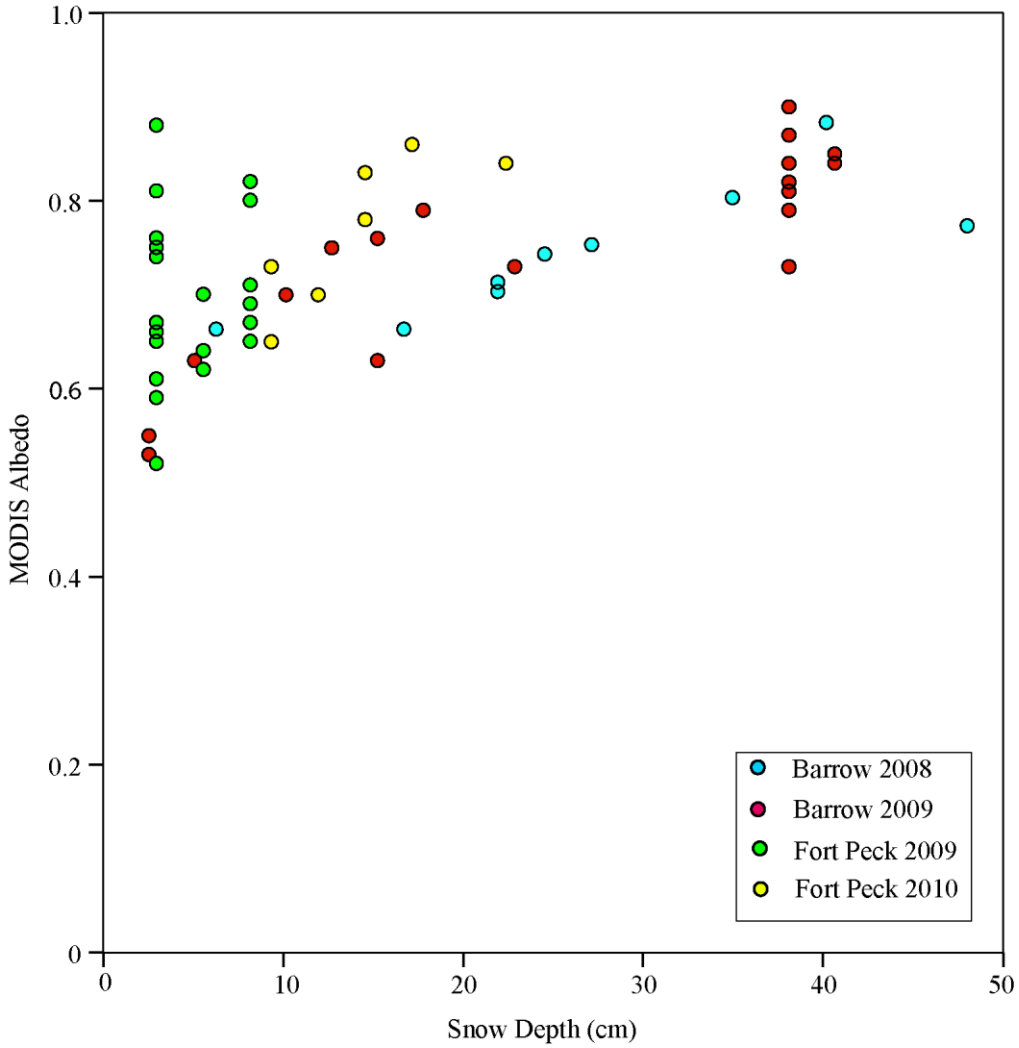

Fig. 43. The relationship between MODIS albedo and snow depth.

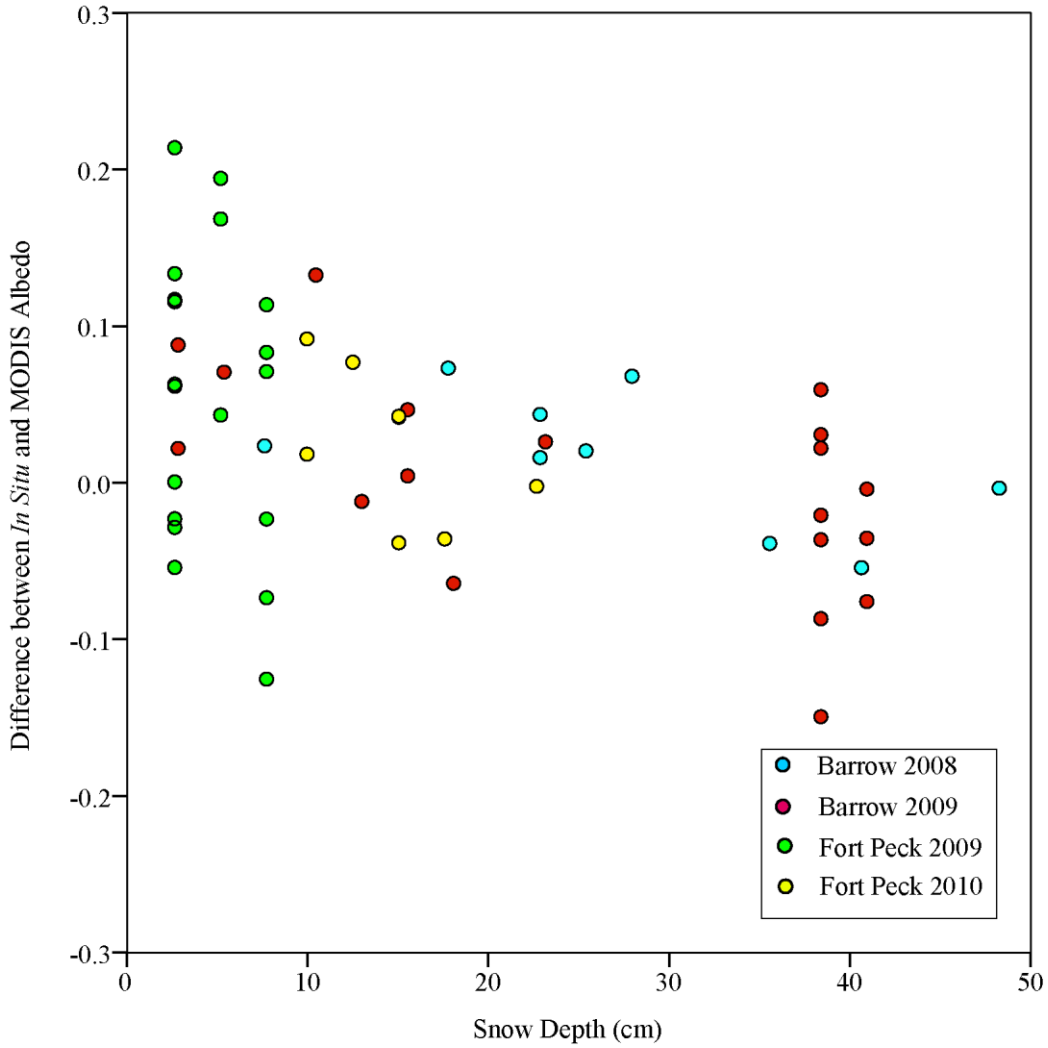

Fig. 44. The relationship between results of *in situ* albedo minus MODIS albedo and snow depth.

5.4 Future Directions

Calibrating the LI-COR measurement is crucial, since using LI-COR is the only practical way to characterize the spatial variations of snow surface albedos.

The station validation time period can be expanded to a decade to examine the accuracy of MOD10A1. Also, as albedo variations are caused by many factors, sufficient

parameters should be examined for their influence on albedo in future research, such as snow depth, snow fraction in a neighboring area etc.

As the spatial representativeness of the two station sites is still not certain, it is worth adapting similar method addressed in this thesis to further check the spatial representativeness over the two stations sites.

6. CONCLUSIONS

In this study the *in situ* validations using different instruments successfully observed the albedo variations both in spatial and in temporal scales. The analysis of these validations show that the *in situ* albedos and the albedos derived from ETM+ and MODIS are quite close, which further demonstrate it is appropriate to use satellite images to derive the snow albedos over very flat and homogeneous areas, such as a frozen lake.

Using geostatistics method to examine the spatial representativeness of snow albedos is a very innovative study. The results show that: (1) one *in situ* measurement of snow albedo over frozen lakes is sufficient enough to characterize the albedos within the range of a MODIS pixel. (2) In most cases, one measurement over snow-covered crop lands of rural regions is sufficient; however, the human impact could reduce the spatial representativeness of an *in situ* measurement.

Station validations also reveal the fact that there is a good correlation between snow albedos retrieved from MODIS and the albedos recorded by ground sensors. The investigation of the relationship between the temperature and albedo changes during snow melting season further demonstrates that the surface albedo is one of the key factors that could significantly influence the earth energy exchange.

In addition, this thesis also shows the feasibility of using a multi-angle mast to measure snow-covered canopy BRDF.

REFERENCES

Aoki, T., Motoyoshi, H., Kodama, Y., Yasunari, T., & Sugiura, K. (2007). Variations of snow physical parameters and their effects on albedo in Sapporo, Japan. *Annals of Glaciology, 46,* 375–281.

ArcGIS desktop help. http://webhelp.esri.com/arcgiSDEsktop/9.3/index.cfm?Topic Name= Semivariograms_and_covariance_functions/ accessed 16th June 2010.

ArcGIS Surface Area and Ratio online manual. http://arcscripts.esri.com /details.asp? dbid=16434/ accessed 10th June 2010.

Atmospheric Radiation Measurement (ARM). https://www.arm.gov/ accessed 1st November 2009.

Brown, G., Bian, L., & Walsh, S.J. (1993). Reponse of a distributed watershed erosion model to variation in input data aggragation levels. *Computer & Geosciences, 19,* 499-509.

Burrough, P.A. (1983). Multiscale sources of spatial variation in soil: The application of fractal concepts of nested levels to soil variation. *Journal of Soil Science, 34,* 577-597.

Burrough, P.A. (1986). *Principles of Geographical Information Systems for Landresources Assessment.* Oxford: Clarendon Press.

Chiles, J. P. & Delfiner, P. (1999). *Geostatististics: Modelling Spatial Uncertainty*. New York: Wiley-Interscience.

Corripio, J. (2004). Snow surface albedo estimation using terrestrial photography. *International Journal of Remote Sensing, 25,* 5705–5729.

Cressie, N. (1993). *Statistics for Spatial Data*. New York: Wiley-Interscience.

Curran, P. J. (1988). The semivariogram in remote sensing: An introduction. *Remote Seising of Environment, 24,* 493-507.

Curtis, B., & Goetz, A. F. H. (1994). Field spectrometry: Techniques and Instrumentation. *Proceedings of an international symposium on Spectral Sensing Research,* San Diego, California, 232-293.

Dorman, J. L., & Sellers, P. J. (1989). A Global Climatology of Albedo, Roughness Length and Stomatal-Resistance for Atmospheric General-Circulation Models as Represented by the Simple Biosphere Model (Sib). *Journal of Applied Meteorology, 28,* 833-855.

Dozier, J., Painter, T. H., Rittger, K., & Frew, J. E. (2008). Time-space continuity of daily maps of fractional snow cover and albedo from MODIS. *Advances in Water Resources, 3,* 1515-1526.

Dozier, J., Green, R., Nolin, A., & Painter, T. (2009). Interpretation of snow properties from imaging spectrometry. *Remote Sensing of Environment, 113,* S25–S37.

Fily, M., Bourdelles, B., Dedieu, J. P., & Sergent, C. (1997). Comparison of in situ and Landsat thematic mapper derived snow grain characteristics in the Alps. *Remote Sensing of Environment, 59,* 452-460.

Frey, R. A., Ackerman, S. A., Liu, Y., Strabala, K. I., & Zhang, H. (2004). Recent improvements in the MODIS cloud mask. *Passive Optical Remote Sensing of the Atmosphere and Clouds, 5652,* 219-230.

Goetz, A. F. H. (1987). The portable Instant Display and Analysis Spectrometer (PIDAS). *Proceeding of the Third Airborne Imaging Spectrometer Data Analysis Workshop*, Pasadena, California, 87-95.

Hahmann, A. N., Ward, D. M., & Dickinson, R. E. (1995). Land-surface temperature and radiative fluxes response of the Ncar Ccm2 biosphere-atmosphere transfer scheme to modifications in the properties of clouds. *Journal of Geophysical Research-Atmospheres, 100,* 23239-23252.

Hall, D.K., Riggs, G.A., Salomonson, V.V., DiGirolamo, N.E., & Bayr, K. J. (2002). MODIS snow-cover products. *Remote Sensing of Environment*, *83,* 181-194.

Hall, D. K., Nghiem, S. V., Schaaf, C. B., DiGirolamo, N. E., & Neumann, G. (2009). Evaluation of surface and nearsurface melt characteristics on the Greenland ice sheet using MODIS and QuikSCAT data. *Journal of Geophysical Research-Earth Surface, 114,* 4006.

Harris, L.D. (1984). *The Fragmented Forest: Island Biogeographic Theory and the Preservation of Biotic Diversity.* Chicago: University of Chicago Press.

Jin, Y. F., Schaaf, C. B., Gao, F., Li, X. W., Strahler, A. H., Lucht, W., & Liang, S. L. (2003). Consistency of MODIS surface bidirectional reflectance distribution function and albedo retrievals: 1. Algorithm performance. *Journal of Geophysical Research-Atmospheres, 108,* 5-10.

Jin, Z., Charlock, T. P., Yang, P., Xie, Y., & Miller, W. (2008). Snow optical properties for different particles shapeswith application to snow grain size retrieval and MODIS/CERES radiance comparison over Antarctica. *Remote Sensing of Environment, 112,* 3563-3581.

Jenness, J. S. (2004). Calculating landscape surface area from digital elevation models. *Wildlife Society Bulletin, 32,* 829-839.

Jenness, J. S. (2009). Surface Area and Ratio for ArcGIS online help. http://www.jennessent.com/arcgis/surface_area.htm/ accessed 19th May 2010.

Jenson, J. R. 2007. *Remote Sensing of the Environment*. New Jercey: Pearson Prentice Hall.

Kimes, D. S., Kirchner, J. A., & Newcomb, W. W. (1983). Spectral radiance errors in remote sensing ground studies due to nearby objects. *Applied optics, 22,* 8-10.

Klein, A. G., Hall, D. K., & Riggs, G. A. (1998). Improving snow cover mapping in forests through the use of a canopy reflectance model. *Hydrological Processes, 12,* 1723-1744.

Klein, A. G., & Stroeve, J. (2002). Development and validation of a snow albedo algorithm for the MODIS instrument. *Annals of Glaciology, 34,* 45-52.

Klein, A. G., & Barnett, A. C. (2003). Validation of daily MODIS snow cover maps of the Upper Rio Grande River Basin for the 2000-2001 snow year. *Remote Sensing of Environment, 86,* 162-176.

Klein, A.G. (2003). Determination of broadband albedos of partially snow-covered sites for validation of MODIS snow albedo retrievals. *Proceedings of 60th Annual Eastern Snow Conference*, Sherbrooke, Quebec, Canada, 120-130.

Krige, D.G. (1951). A statistical approach to some mine valuations and allied problems at the Witwatersrand. *Master's thesis of the University of Witwatersrand* accessed 10th May 2010.

Li, D., Jie, S., & Gong, J. (2009). *Geospatial Technology for Earth observation*. New Jersey: Springer.

Liang, S. L., Strahler, A. H., & Walthall, C. (1999). Retrieval of land surface albedo from satellite observations: A simulation study. *Journal of Applied Meteorology, 38,* 712-725.

Liang, S. L. (2001). Narrowband to broadband conversions of land surface albedo I Algorithms. *Remote Sensing of Environment, 76,* 213-238.

Liang, S. L., H. Fang, M., Chen, C. J., Shuey, C., Walthall, C., Daughtry, J., Morisette, C., Schaaf, S., & Strahler, A. (2002). Validating MODIS land surface reflectance and albedo products: methods and preliminary results. *Remote Sensing of Environment, 83,* 149-162.

Liang, S. L., Shuey, C. J., Russ, A. L., Fang, H. L., Chen, M. Z., Walthall, C. L., Daughtry, C. S. T., & Hunt, R. (2003). Narrowband to broadband conversions of land surface albedo: II. Validation. *Remote Sensing of Environment, 84,* 25-41.

Liang S. L. (2004). *Quantitative Semote Sensing of Land Surfaces.* New York: Wiley-Interscience.

Lofgren, B. M. (1995). Surface Albedo Climate Feedback Simulated Using 2-Way Coupling. *Journal of Climate, 8,* 2543-2562.

Longley P., Goodchild, M. F., Maguire, D. J., & Rhind, D. W. (2004). *Geographic Information Systems and Science.* New York: Wiley-Interscience.

Lucht, W., Schaaf, C. B., & Strahler, A. H. (2000). An algorithm for the retrieval of albedo from space using semiempirical BRDF models. *Ieee Transactions on Geoscience and Remote Sensing, 38,* 977-998.

Mandelbrot, B.B. (1982). *The Fractal Geometry of Nature.* New York: W.H. Freeman and Company.

Manninen, S. (2009). Simulation of the effect of snow covered forest floor on the total forest albedo. *Algriculture and Forest Meteorology, 149,* 303-319.

Matheron, G. (1971) The Theory of Regionalized Variables and Its Applications. Paris: Mines Paris Tech.

McGarigal, K., McComb, W.C. (1995). Relationships between landscape structure and breeding birds in Oregon Coast Range. *Ecological Monographs, 65,* 235-260.

McGarigal, K. (1995). FRAGSTATS: Spatial Pattern Analysis Program for Quantifying Landscape Structure. http://www.umass.edu/landeco/research/fragstats/fragstats.html/ accessed 19th May 2010.

Meentemeyer, V. (1989). Geographical perpectives of space, time and scale. *Landscape ecology, 3,* 163-173.

Milne, B.T. (1988). Measuring the fractal geometry of landscapes. *Applied Mathematics and Computation, 27,* 67-79.

Milton E., Schaepman M. E., Anderson K., Kneubühler M., & Fox N. (2009). Progress in field spectroscopy. *Remote Sensing of Environment, 113,* S92–S109.

NASA (2009). Landsat 7. Science Data Users Handbook http://landsathandbook.gsfc.nasa.gov/handbook.html/ accessed 17th May 2010.

NOAA SURFRAD network. http://www.srrb.noaa.gov/surfrad/ accessed 13rd November 2009.

NOAA GMD network. whttp://www.esrl.noaa.gov/gmd/grad/field.html/ accessed 13rd November 2009.

Oerlemans, J. & Knap, W. (1998). A 1 year record of global radiation and albedo in the ablation zone of Morteratschgletsher,Switzerland. *Journal of Glaciology, 44,* 231–238.

Peltoniemi J., Kaasalainen S., Naranen J. Rautiainen M., Stenberg P., Smolander H., Smolander S., & Voipio P. (2005). BRDF measurement of understory vegetation in pine forests: dwarf shrubs, lichen, and moss. *Remote Sensing of Environment, 94,* 343-354.

Penndorf, R. (1956). Luminous and spectral reflectance as well as colors of natural objects. U.S. Air Force Cambridge Research Center, Bedford, Massachusetts. Accessed 20th May 2010.

Ranson, K. J., Irons, J. R., & Williams, D. L. (1994). Multispectral bidirectional reflectance of northern forest canopies with the advanced Solid-State Array Spectroradiometer (Asas). *Remote Sensing of Environment, 47,* 276-289.

Ricciardelli, E., Romano, F., & Cuomo, V. (2010). A technique for classifying uncertain MOD35/MYD35 pixels through meteosat second generation-spinning enhanced visible and infrared imager observations. *Ieee Transactions on Geoscience and Remote Sensing, 48,* 2137-2149.

Risser, P. G., Karr, J. R., & Forman, R.T. (1984). *Landscape Ecology: Directions and Approaches.* Illinois: Illinois Natural History Survey.

Schaaf, C. B., Gao, F., Strahler, A. H., Lucht, W., Li, X. W. et al., (2002). First operational BRDF, albedo nadir reflectance products from MODIS. *Remote Sensing of Environment, 83,* 135-148.

Schaepman-Strub, G., Schaepman, M. E., Painter, T. H., Dangel, S., & Martonchik, J. V. (2006). Reflectance quantities in optical remote sensing—definitions and case studies. *Remote Sensing of Environment, 103,* 27-42.

Sorman, A. U., Akyurek, Z., Sensoy, A., Sorman, A. A., and Tekeli, A. E. (2006). Commentary on comparison of MODIS snow cover and albedo products with ground observations over the mountainous terrain of Turkey. *Hydrology and Earth System Science, 3,* 3655– 3673.

Stamnes, K., Tsay, S. C., Wiscombe, W., & Jayaweera, K. (1988). Numerically Stable Algorithm for Discrete-Ordinate-Method Radiative-Transfer in Multiple-Scattering and Emitting Layered Media. *Applied Optics, 27,* 2502-2509.

Stroeve, J., Nolin, A., & Steffen, K. (1997). Comparison of AVHRR-derived and in situ surface albedo over the Greenland ice sheet. *Remote Sensing of Environment, 62,* 262-276.

Stroeve, J. Box, J. E., Fowler, C., Haran, T., & Key, J. (2001). Intercomparison between in situ and AVHRR polar pathfinder-derived surface albedo over Greenland. *Remote Sensing of Environment, 75,* 360-374.

Stroeve, J. C., & Nolin, A. W. (2002). New methods to infer snow albedo from the MISR instrument with applications to the Greenland ice sheet. *IEEE Transactions on Geoscience and Remote Sensing, 40,* 1616-1625.

Stroeve, J., Box, J. E., Gao, F., Liang, S. L., Nolin, A., & Schaaf, C. (2005). Accuracy assessment of the MODIS 16-day albedo product for snow: comparisons with Greenland in situ measurements. *Remote Sensing of Environment, 94,* 46-60.

Stroeve, J. C., Box, J. E., & Haran, T. (2006). Evaluation of the MODIS (MOD10A1) daily snow albedo product over the Greenland ice sheet. *Remote Sensing of Environment, 105,* 155-171.

SURFRAD Network FTP. ftp://ftp.srrb.noaa.gov/pub/data/surfrad/Fort_Peck_MT/ accessed 14th November 2010.

Tekeli, A. E., Ensoy, A., Sorman, A., Akyurek, Z., & Sorman, U. (2006). Accuracy assessment of MODIS daily snow albedo retrievals with in situ measurements in Karasu basin, Turkey. *Hydrological Processes, 20,* 705-721.

USGS Global Visualization (GloVis) data inventory tool. http://glovis.usgs.gov/ accessed 2nd January 2010.

Vermonte, E.F., & Kotchenova, S.Y. (2008). MOD09 (Surface Reflectance) User's Guide, Version 1.1. http://modiss r.ltdri.org/MAIN_SURFACE_PRO DUCTAND%20 USER%20GUIDE/MOD09_UserGuide.pdf/ accessed 15th January 2010.

Walsh, S. J., Evans, T. P., Welsh, W. F., Entwisle, B., & Rindfuss, R. B. (1999). Scale-dependent relationships between population and environment in N. E. Thailand. *Photogrametric Engineering & Remote Sensing, 65,* 97-105.

Warehouse Inventory Search Tool (WIST). https://lpdaac.usgs.gov/lpdaac/get_data/wist/ accessed 12nd November 2009.

Warren, S. G. (1982). Optical properties of snow. *Reviews of Geophysics and Space Physics, 20,* 67–89.

Wu, A., Li, Z., & Cihlar, J. (1995). Effects of land cover type and the greenness on advanced very high resolution radiometer bidirectional reflectance: analysis and removal. *Journal of Geophysical Research, 100,* 9179-9192.

Yu, Y., Chen, H. B., Xia, X. G., Xuan, Y. J., & Yu, K. (2010). Significant variations of surface albedo during a snowy period at Xianghe observatory, China. *Advances in Atmospheric Sciences, 27,* 80-86.

VITA

Name:
Panshu Zhao

Address:
Texas A&M University
707G O&M Building, TAMU Mail Stop 3147
College Station, TX 77843

Email Address:
rochesterzhao@gmail.com

Education:
B.A., GIS, Nanjing University of Posts & Telecommunications, 2009
M.S., Geography, Texas A&M University, 2012

Research Interest:
GIS, Remote Sensing

Poster Presentations:

Zhao, P. and Klein, A.G. In situ validation and relevant analysis of snow albedo derived from ETM+ and MODIS images, Spirit Lake, Iowa. *Annual Meeting of the Association of the Southwestern American Geographers*, Northeastern State University, Tahlequah, Oklahoma, October 14-16, 2010.

Zhao, P. and Klein, A.G. Investigating the spatial representativeness of snow albedos derived from multiple remote sensing sensors. *Annual Meeting of the Association of the American Geographers*, Seattle, Washington, April 11-16, 2011.

Zhao, P. and Klein, A.G. Investigating the spatial representativeness of snow albedos through remote sensing and geostatistics. *The 68th Annual Eastern Snow Conference*, Montreal, Quebec, Canada, June 14-17, 2011.